

Fictitious Play in 3×3 Games: the transition between periodic and chaotic behaviour *

Colin Sparrow[†], Sebastian van Strien[‡], Christopher Harris[§]

April 25, 2006

Abstract

In the 60's Shapley provided an example of a two player fictitious game with periodic behaviour. In this game, player A aims to copy B 's behaviour and player B aims to play one ahead of player A . In this paper we generalize Shapley's example by introducing an external parameter, and showing that the periodic behaviour in Shapley's example at some critical parameter value disintegrates into unpredictable (chaotic) behaviour, with players dithering a huge number of times between different strategies. At a further critical parameter the dynamics becomes periodic again and both players aim to play one ahead of the other. In this paper we adopt a geometric (dynamical systems) approach and show that GENERICALLY the dynamics of fictitious play is essentially continuous and uniquely defined everywhere except at the interior equilibrium. In this paper we shall concentrate on the periodic behaviour, while in the sequel to this paper we shall describe the chaotic behaviour in more detail.

1 Introduction

Suppose that a two-player finite game in normal form is repeated infinitely often. Suppose further that, at each stage of the repeated game, each player plays a best response to the empirical distribution of the past play of her opponent. Then the state of the repeated game at any given stage can be summarized by the pair consisting of the empirical distribution of past actions of player A and the empirical distribution of past actions of player B , and this state evolves according to a dynamical system. This dynamical system is known as fictitious play.

Fictitious play arises in many different guises in economics. It was originally proposed as an algorithm for finding equilibrium.¹ It was later reinterpreted as a model of boundedly rational learning in interactive settings.² Several modifications have been introduced, including: (i) a modification in which players do not play exact best responses but instead choose actions with a

*The first draft of this paper was written in 1999 when Colin Sparrow was on a sabbatical leave from Cambridge visiting Warwick

[†]csparrow@maths.warwick.ac.uk

[‡]strien@maths.warwick.ac.uk

[§]Department of Economics, Cambridge. cjh22@cus.cam.ac.uk

¹See Brown [1949], [1951a] and [1951b].

²See Chapter 2 of Fudenberg & Levine [1998] and the references cited there.

probability that increases with their payoffs;³ (ii) a modification in which each player is replaced by a population of players whose payoffs differ by a small random perturbations;⁴ and (iii) a modification in which players play exact best responses with some probability and experiment at random with some probability.⁵ Finally, there is a discrete-time version, in which the underlying normal-form game is played for each $t \in \{0, 1, 2, \dots\}$, and a continuous-time version, in which the underlying normal-form game is played for each $t \in [0, +\infty)$.

Much effort has been devoted to finding sufficient conditions under which fictitious play converges to an equilibrium from all starting points. For example, fictitious play has been shown to converge in: (i) zero-sum games;⁶ (ii) generic $2 \times n$ nonzero-sum games;⁷ (iii) potential games;⁸ (iv) dominance-solvable games;⁹ and (v) various classes of supermodular games.¹⁰

Some effort has also been devoted to understanding fictitious play in games in which fictitious play does not necessarily converge to an equilibrium. The first contribution to this strand of the literature was made by Shapley [1964], who identified a generic 3×3 nonzero-sum game for which fictitious play has a stable limit cycle. Three more recent contributions are: Jordan [1993], who constructed a $2 \times 2 \times 2$ game for which fictitious play has a stable limit cycle; Gaunersdorfer & Hofbauer [1995], who established an interesting relationship between the replicator dynamics and fictitious play in three examples in which fictitious play converges to a limit cycle (namely Shapley's example, Jordan's example and the rock-scissors-paper game); and Cowan [1992], who identified a difficult numerical example in which fictitious play exhibits chaotic behaviour (in the sense that the flow contains a subshift of finite type).

In this and a sequel to this paper we shall show make a detailed analysis of the following family of 3×3 games with utilities v^A and v^B determined by the matrices

$$A = \begin{pmatrix} 1 & 0 & \beta \\ \beta & 1 & 0 \\ 0 & \beta & 1 \end{pmatrix} \quad B = \begin{pmatrix} -\beta & 1 & 0 \\ 0 & -\beta & 1 \\ 1 & 0 & -\beta \end{pmatrix}, \quad (1.1)$$

which depend on a parameter $\beta \in (-1, 1)$ (and best response dynamics given by the differential inclusion (2.2)). For $\beta = 0$, this game is equal to Shapley's: irrespective of the starting position, every orbit tends to a periodic motion, with eventually player A copying the previous move of player B , while player B is aiming to play one ahead from the previous move of player A . Plotting the index of the largest component of the utilities v^A and v^B ("the strategy" of player A resp. B) as a function of time we obtain the repeating pattern (repeating in 6 steps):

time duration	0.33123	0.31767	0.33123	0.31767	0.33123	0.31767
strategy player A	1	2	2	3	3	1
strategy player B	2	2	3	3	1	1

³See Cowan [1992] and Fudenberg & Levine [1995].

⁴See Ellison & Fudenberg [1998].

⁵See Fudenberg & Levine [1998] and the references cited there.

⁶See Robinson [1951], Hofbauer [1995] and Harris [1998].

⁷See: Miyasawa [1961] and Metrick & Polak [1994] for the 2×2 case; Sela [1998] for the 2×3 case; and Berger [2005] for the general case.

⁸See Monderer & Shapley [1996] for the case of weighted potential games and Berger [2003] for the case of ordinal potential games.

⁹See Milgrom & Roberts [1991].

¹⁰See: Krishna [1992] for the case of supermodular games with diminishing returns; Hahn [1999] for the case of 3×3 supermodular games; and Berger [2003] for the case of quasi-supermodular games with diminishing returns, the case of quasi-supermodular $3 \times n$ games and the case of quasi-supermodular 4×4 games.

That is, during 0.33123 time units players A, B prefer strategies 1, 2 respectively, then for 0.31767 time units they prefer 2, 2 and so on.

For $\beta = 1$ the players' game also tends to a periodic pattern, but now both player A and B aim to play one ahead from the other player, and therefore now infinitely often repeat (again repeating in 6 steps):

time duration	0.12060	0.39493	0.12060	0.39493	0.12060	0.39492
strategy player A	1	1	3	3	2	2
strategy player B	3	2	2	1	1	3

We call this the *anti-Shapley* pattern. The main point of this paper is to show how this change of behaviour occurs. It turns out that there are two *critical* parameters, σ the golden mean ≈ 0.618 and $\tau \approx 0.915$ such that

- for $\beta \in (-1, \sigma)$ the players typically end up repeating Shapley's pattern; in fact, for $\beta \in (-1, 0]$ regardless of the initial positions, the behaviour tends to a periodic one (for $\beta > 0$ this is not true: then there are orbits which tend to the interior equilibrium and/or other periodic orbits).
- for $\beta \in (\sigma, \tau)$ the players become extremely indecisive and erratic (and the moves become chaotic), while
- for $\beta \in (\tau, 1)$ the players typically end up playing the anti-Shapley pattern.

For example, when $\beta = 0.75$ one sees behaviour such as

```

strat. A  331122233112211322333223322133113331133113311331133211221122
strat. B  2112213311223322233211331133311332112211221122112211221
```

In this paper we shall describe the bifurcations that the periodic orbits undergo as β varies; in a sequel to this paper [2006] the nature of the chaotic motion will be described in more detail (for example, that even for $\beta \in (0, \sigma)$, there are many (exceptional) orbits that are attracted to the equilibrium point).

Of course, when one or more of the players is indifferent between two strategies their dynamics is not uniquely determined. However, as we shall show in Corollary 2.1 (in Subsection 2.1) under a mild assumption *only exceptional* orbits of the play are affected by this ambiguity. In particular, the orbits discussed above are uniquely determined.

2 Continuous Time Fictitious Play: the Generic Case

We study the following version of continuous time fictitious play, which is convenient for calculation, for numerical simulation, and for extracting the geometrical properties of the dynamics. It is equivalent to other formulations in the literature. Two players A and B , both having n strategies to choose from, have $n \times n$ pay-off matrices $A = (a_{ij})$ and $B = (b_{ij})$, $1 \leq i, j \leq n$ respectively. (The context will always make it clear whether we are talking about Players A or B or about the matrices A and B). We will assume throughout this paper that the matrices A and B are both *non-singular* (i.e. have non-zero determinant). We denote the set of probability vectors for players A and B by $\Sigma_A, \Sigma_B \subset \mathbb{R}^n$. (Though both simplices are the same subset

of \mathbb{R}^n , the subscripts are useful when we wish to make it clear which players probabilities we are discussing). At some time $t_0 \in \mathbb{R}$ the *state* of the game is given by a pair of probability vectors, $(p^A(t_0), p^B(t_0)) \in \Sigma := \Sigma_A \times \Sigma_B$, representing the current (usually mixed) strategies of the two players. It is convenient to define p^A and p^B so that they are row and column vectors respectively.

The dynamics of the system is determined as follows. At time t_0 , each player computes a *best response* $BR_A(p^B) \in \Sigma_A$ and $BR_B(p^A) \in \Sigma_B$ to the other player's current strategy. If we denote the set of pure strategies for the two players by $P_i^A \in \Sigma_A$ and $P_j^B \in \Sigma_B$, $1 \leq i, j, \leq n$, then generically ¹¹ player A's best response BR_A is a pure strategy $P_i^A \in \Sigma_A$, for some $i \in \{1, \dots, n\}$ chosen so that the i -th coordinate of the vector

$$v^A(t_0) = Ap^B(t_0)$$

is larger than the other coordinates (the non-generic case, when several coordinates of the vector $v^A(t_0)$ are equal will be treated later on). Similarly, player B's best response BR_B is generically a pure strategy $P_j^B \in \Sigma_B$, $j \in \{1, \dots, n\}$ where j is chosen so that the j -th coordinate of the vector

$$v^B(t_0) = p^A(t_0)B$$

is larger than any of the other coordinates. In cases where players are indifferent between two or more strategies (the non-generic case), any convex combination of the relevant pure strategies is an equally good best response, so

$$BR_A: \Sigma_B \rightarrow \Sigma_A \text{ and } BR_B: \Sigma_A \rightarrow \Sigma_B$$

are in fact *set-valued maps*. This means equation (2.2) below actually defines a differential inclusion rather than a differential equation. ¹²

Once best responses are selected, the dynamics is determined by the piecewise linear equations:

$$\begin{aligned} dp^A/dt &= BR_A(p^B) - p^A \\ dp^B/dt &= BR_B(p^A) - p^B \end{aligned} \tag{2.2}$$

so that each player's tendency is to adjust their strategy in a straight line from their current strategy towards their current best response. In the GENERIC case as discussed above, player A continuously adjusts her probability vector $p^A(t)$ from its current position $p^A(t_0)$ in a straight line towards P_i^A , and player B similarly adjusts $p^B(t)$ to move in a straight line towards P_j^B , so that for times greater than t_0 , and for so long as strategies P_i^A and P_j^B remain unique best responses, we may write, after a reparameterisation of time, the solution of (2.2) becomes

$$\begin{aligned} p^A(t_0 + s) &= p^A(t_0)(1 - s) + s \cdot P_i^A, \\ p^B(t_0 + s) &= p^B(t_0)(1 - s) + s \cdot P_j^B, \end{aligned} \tag{2.3}$$

for $s \in [0, 1]$. Note that we have parameterised time so that both players move towards their best response strategies at a uniform speed, such that if their best responses did not change they

¹¹In this paper the word 'generic' means that one is not in a codimension-one subspace

¹²We will deal with this apparent complication in sections 2.1 and 2.2 below. Our approach will be to consider the flow where best responses *are* uniquely defined and to investigate the extent to which this flow extends in a unique and continuous way onto the parts of phase space where best responses are not unique; for the moment readers unfamiliar with the idea of differential inclusion will lose very little by continuing to think of (2.2) as a differential equation.

would arrive at $(P_i^A, P_j^B) \in \partial\Sigma$ at time $t = t_0 + 1$, at which point the dynamics would halt. The parameterisation is chosen for ease of calculation and computation, and does not affect the geometry of the dynamics which is our chief concern in this paper; it would be straightforward to use the original time $\varrho = -\ln(1-s)$ if an exponential approach to (P_i^A, P_j^B) in infinite time were preferred (the speed of a solution of (2.2) is proportional to the distance to the target point). In any case, since orbits consist of pieces of line segments, numerical simulations can be done easily and with arbitrary accuracy.

Equations (2.3) therefore determine the dynamics up *until such time* as one or other (or both) players become *indifferent* between two (or more) pure strategies.

Let us first describe the sets where the best responses are constant. We will be particularly interested in games where there is an *interior equilibrium*; that is a point $E = (E^A, E^B)$ in the interior of $\Sigma_A \times \Sigma_B$ where both players are indifferent between *all* n strategies, so that all components of Ae^B are equal, and all components of $e^A B$ are equal. The following lemma is entirely straightforward.

Lemma 2.1 (The complement of the indifferent sets). *Assume that A and B are $n \times n$ non-singular matrices. Then the set where one player is indifferent between two given strategies (and so where she has a choice of best responses) forms a codimension-one hyperplane and for each $1 \leq i, j \leq n$ the set*

$$S_{ij} = \{(p^A, p^B) ; BR_A(p^B) = P_i^A \text{ and } BR_B(p^A) = P_j^B\}$$

is convex.

If there exists an equilibrium $E = (E^A, E^B)$ in the interior of Σ , then all n^2 regions S_{ij} are non-empty, and their closures meet at (E^A, E^B) .

Figure 1 shows a 3×3 example in which the two simplices Σ_A and Σ_B are each two dimensional triangles, with vertices representing the pure strategies of the two players as labelled, and the regions S_{ij} with different aims marked in the figure. The state of the system at a particular time, $(p^A(t), p^B(t))$ is represented by a pair of points, p^A and p^B , one in each simplex. The local direction of motion is towards the vertex determined by the location of the other players position in her simplex, as illustrated. Motion will continue in a straight line until one or other player hits an indifference line (see caption).

2.1 Uniqueness and continuity of dynamics where at most one player is indifferent

We now consider, for general matrices A and B , the hyperplanes where one or other player is indifferent between two strategies.

Let us denote the set where player A is indifferent between strategies P_i^A and P_j^A by $Z_{i,j}^A \subset \Sigma_B$. We define $Z_{i,j}^B \subset \Sigma_A$ similarly. If we set $Z^A = \cup_{i,j} Z_{i,j}^A$, then $\Sigma_A \times Z^A$ is the set where player A does not have a unique best response. We define the set Z^B similarly. Outside the set

$$Z = (\Sigma_A \times Z^A) \cup (Z^B \times \Sigma_B)$$

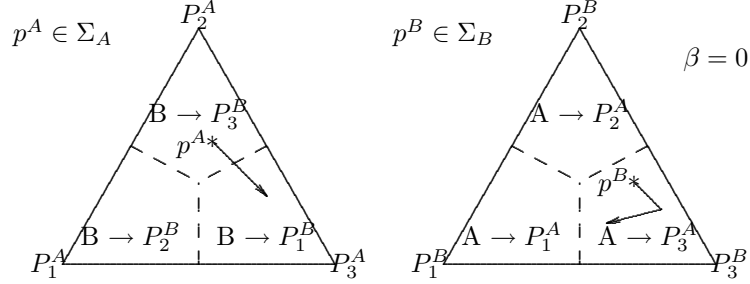


Figure 1: An example in which the simplices Σ_A and Σ_B the regions where players have a specific preference are as shown, separated by dashed lines which show the indifference sets $Z^B \subset \Sigma_A$ where player B is indifferent between two or more strategies, and $Z^A \subset \Sigma_B$ where player A is indifferent between two or more strategies. Starting from an initial condition (p^A, p^B) (marked with the * symbols), player A moves towards P_3^A , while Player B starts by moving towards P_3^B and changes direction towards P_1^B as p^A crosses Z^B . The sets $S_{ij} \in \mathbb{R}^4$ are the sets formed as products of two kite-shaped regions where each player has a strict preference.

where at least one of the players is indifferent between two or more strategies the flow is uniquely defined by (3.7) and is clearly continuous. If we define

$$Z^* = Z^B \times Z^A \subset \Sigma_A \times \Sigma_B, \quad (2.4)$$

which is the subset of Z where *both* players are indifferent between at least two strategies, then the next lemma says that the uniqueness and continuity extends to the *complement* of Z^* providing matrices A and B satisfy the condition (2.5) in the lemma. (Note that this transversality condition is satisfied for the Shapley example from above if and only if $\beta \neq 0$.)

Proposition 2.1 (Transversality condition implies some continuity). *The motion defined by equations (2.2) forms a continuous flow on $(\Sigma_A \times \Sigma_B) \setminus Z^*$ provided the following condition is met: for any point $(p^A, p^B) \notin Z^*$ with, say, $p^A \in Z^B$, $p^B \notin Z^A$ and strategy P_k^A preferable for player A,*

$$\text{the vector } P_k^A \text{ is not parallel to the plane } Z^B \subset \Sigma_A \text{ at } p^A \quad (2.5)$$

(and similarly, in the case when the role of p^A and p^B is reversed).

Proof. The transversality condition (2.5) ensures that a point is moved immediately off the codimension-one plane $Z^B \times \Sigma_B$ so that player B has a unique best response the moment the motion begins. \square

Since Z^* has zero Lebesgue measure and consists of codimension two planes, this shows

Corollary 2.1. *Assume the transversality condition (2.5) holds. Then there exists a set $X \subset \Sigma_A \times \Sigma_B$ of initial conditions such that*

- for each starting point in X the flow defined by (2.2) is continuous and unique for all $t \geq 0$.
- X has full Lebesgue measure and is open and dense.

2.2 The dynamics nearby the set where both players are indifferent

Even though the previous corollary shows that most starting positions never enter the set Z^* where both players are indifferent, it is still important to analyse the dynamics *near* this set. As it turns out, in many places the flow outside Z^* extends continuously to Z^* . This suggests a natural choice of the non-uniquely defined dynamics within Z^* . Much more importantly - even if we are not interested in orbits that lie on Z^* and do not want to make a choice for the dynamics on this set - the continuous extension dynamics on Z^* is an “organising principle” for nearby orbits, as we shall see below. This continuous extension dynamics makes that all orbits near Z^* have consistent dynamics. This point of view puts us in a classical dynamical systems framework and allows us, for example, to describe bifurcations of the flow (i.e. changes in dynamics when the parameter β changes) for orbits near Z^* (as we shall see in the Section 3).

Before going to the general case, let us first review the dynamics in the 2×2 case (this of course is well known, but it is useful to be explicit here as we shall use the classification later on). In this case the probability vectors Σ_A and Σ_B in \mathbb{R}^2 can both be identified with $[0, 1]$ and so $\Sigma_A \times \Sigma_B$ with the square $[0, 1] \times [0, 1]$. Player A moves left or right, depending on the position of player B , i.e. depending whether (Σ_A, Σ_B) is above or below a certain horizontal line, and similarly player B moves up or down depending on whether (Σ_A, Σ_B) is to the left or right of some vertical line. Drawn in Figure 2 are a few orbits of the system in various cases and \bullet marks the aims $(0, 0)$, $(1, 0)$, $(0, 1)$ and $(1, 1)$. The dotted lines denote where one player is indifferent to two strategies. From left to right cases (1), (2), (3), (2) and (3). In cases (2) the orbit spirals towards the interior point, while in case (3) the interior point acts as a saddle.

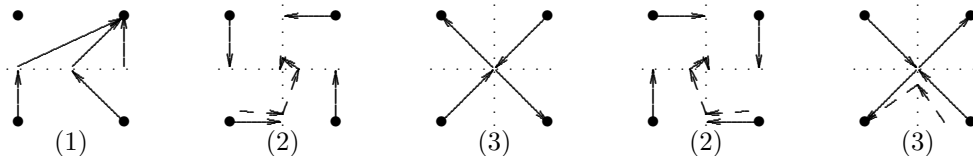


Figure 2: The motion in various cases for 2×2 games.

Lemma 2.2 (2×2 case). *Assume that both players have two strategies and that the corresponding 2×2 matrices are non-singular. Then there are three possibilities:*

1. *there is no interior equilibrium in $\Sigma_A \times \Sigma_B$ and all orbits tend to a unique singular point on the boundary (this occurs if Z^A and or Z^B are empty, and is depicted in (1) in Figure 2);*
2. *there is an interior equilibrium E which is stable, orbits spiral towards it and the flow extends continuously to E (this is depicted in (2) in Figure 2);*
3. *there is an interior equilibrium E which is a saddle point and the flow cannot be extended in a continuous way to E and there is genuine non-uniqueness in the flow near E (this is depicted in (3) in Figure 2).*

As we shall see in the next section, in case (2) the solution tends to E as $t \rightarrow \infty$, spiralling faster and faster around E in a very precise way. This means that we can think of the flow at E as just stationary there.

We now consider the behaviour of the system when both players are indifferent between two or more strategies (but now for general A and B). This occurs on the set $Z^* = Z^B \times Z^A$ defined above. Since we are interested in typical trajectories of the system, and typical trajectories will not actually hit Z^* , we are particularly concerned with the implications of this for trajectories near to but not on Z^* . This contrasts with the case of the codimension one sets considered above; typical trajectories do hit those. We will see, though, that we can in many circumstances define a unique flow for points in Z^* as well.

Consider the subset $Z'_{kl,ij}$ of $Z^B_{k,l} \times Z^A_{i,j} \subset Z^*$ where player A is indifferent *only* between strategies i and j , and player B is indifferent *only* between strategies k and l . Since we assumed that A and B are non-singular, this is a codimension-two plane in $\Sigma_A \times \Sigma_B$. Define a neighbourhood of $Z'_{kl,ij}$ by

$$N = \{(p^A, p^B) ; BR_A(p^B) \subset \{i, j\} \text{ and } BR_B(p^A) \subset \{k, l\}\}. \quad (2.6)$$

In the set N , player A prefers strategies i and j to all other pure strategies, and player B prefers strategies k and l . In $N \setminus Z'$, because of Proposition 2.1 above, equation (2.2) can be justifiably interpreted as a differential equation with unique solutions (rather than a differential inclusion with possibly non-unique solutions) with the dynamics consisting of a linear decline in all components $p_m^A, m \neq i, j$ and $p_n^B, n \neq k, l$ while the behaviour of the other two components of p^A and p^B depends entirely on the 2×2 submatrices of A and B :

$$A[k, l] = \begin{pmatrix} a_{k,k} & a_{k,l} \\ a_{l,k} & a_{l,l} \end{pmatrix} \quad B[i, j] = \begin{pmatrix} b_{i,i} & b_{i,j} \\ b_{j,i} & b_{j,j} \end{pmatrix}.$$

These matrices describe a game on the two-dimensional space spanned by $[P_i^A, P_j^B] \times [P_k^B, P_l^B]$ (where $[P_i^A, P_j^A]$ stands for the line segment $\lambda P_i^A + (1 - \lambda)P_j^A \subset \Sigma_A, 0 \leq \lambda \leq 1$). It follows that the dynamics in N is the product of the dynamics in this two-dimensional space (on which the dynamics is as in Figure 2) and a linear decline along the codimension-two plane in Z' . Together with Lemma 2.1 this gives:

Proposition 2.2 (Continuity and uniqueness outside sets of codimension three). *Assume that A and B are non-singular and that the transversality condition (2.5) is satisfied. Then the flow defined on the sets S_{ij} has a unique continuous extension everywhere except (possibly) where:*

- *one player is indifferent to at least three strategies and the other to at least two;*
- *both players are indifferent to precisely two strategies and along this set the dynamics is as in case (3) described above (in Lemma 2.2).*

In the neighbourhood N of $Z'_{kl,ij}$ defined in (2.6) the flow decomposes into a flow governed by a two by two game, and a constant flow in the remaining direction(s) and there are three cases:

1. *trajectories cross either $Z^B_{k,l}$ or $Z^A_{i,j}$ and locally the flow is the product of a constant flow perpendicular to the plane and a flow as in (1) in Figure 2;*
2. *trajectories in N spiral towards 0 (i.e. towards Z') along a cone over a quadrangle as in Figure 3, and move closer and closer to the unique trajectory in Z' that remains in Z' - this trajectory is therefore the unique continuous extension of the flow in N onto Z' - and locally the two-dimensional flow is as in (2) in Figure 2;*

3. Z' acts as a saddle and generic trajectories leave N moving away from Z' in one of two opposite directions and locally the two-dimensional flow as in (3) in Figure 2.

Proof. Only the 2nd case needs some explanation. Let S be the two dimensional plane spanned by the four targets (P_s^A, P_t^B) , $s \in \{i, j\}$ and $t \in \{k, l\}$. Moreover let $V \subset S$ be a quadrangle with sides parallel to the lines connecting the equilibrium $E \in S$ to (P_s^A, P_t^B) , $s \in \{i, j\}$ and $t \in \{k, l\}$ (in such a way that in the region where the players aim for (P_s^A, P_t^B) one takes a line parallel to the line connecting E to (P_s^A, P_t^B)). Now taking any quadrangle V_r parallel to V , and the cone through the equilibrium $E \in S$ over V_r . Clearly orbits that start in this cone, will stay in it. \square

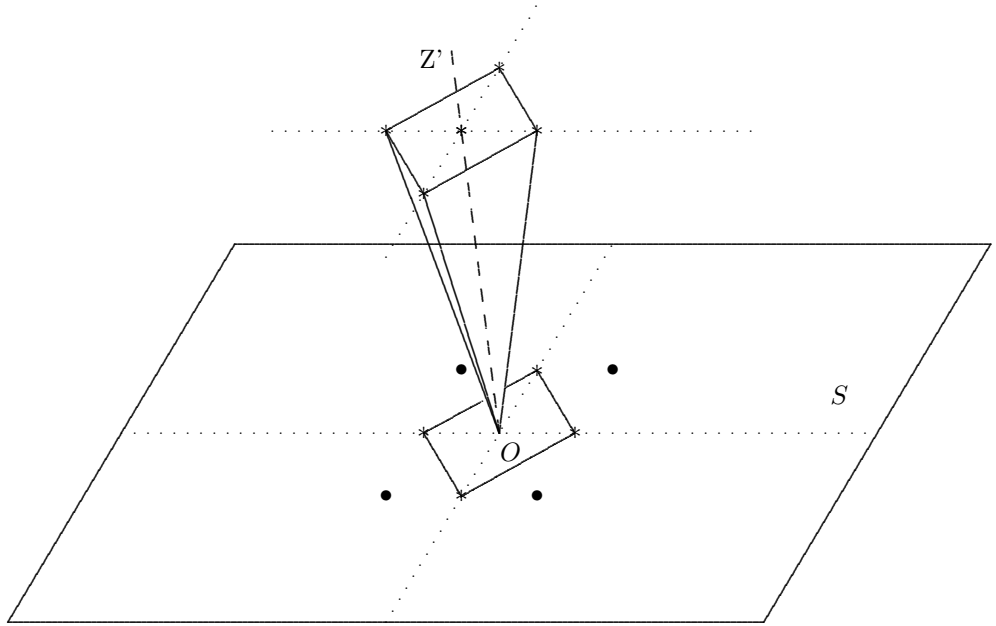


Figure 3: The targets (P_s^A, P_t^B) , $s \in \{i, j\}$, $t \in \{k, l\}$ in the plane S are drawn marked as \bullet . The dashed line corresponds to Z . A quadrangle T_r in S is also drawn and also another quadrangle T'_r which is in a plane S_q (through $q \in Z$) which is parallel to S is drawn. The cone of the quadrangle over the equilibrium point E is invariant. Orbits spiral along the cone towards O , always aiming for one of the points marked as \bullet . Note that the motion on the cone is **not** close to the direction of the axis Z' .

The above geometrical analysis gives a slightly different (though equivalent) slant on the behaviour on Z^* to that obtained in the more usual way by emphasizing that the best response functions BR_A and BR_B as set valued functions. In that point of view we are forced to emphasize that for player A at $(p^A, p^B) \in Z_{k,l}^B \times Z_{i,j}^A$ as above, any response $\lambda P_i^A + (1 - \lambda)P_j^A$, $0 \leq \lambda \leq 1$ is a best response, and similarly for player B. This seems to imply genuine non-uniqueness of the flow at all points (p^A, p^B) in Z^* . In fact, in case (1) though both players have a choice of best response at (p^A, p^B) , there is no choice of best responses that keeps the trajectory inside Z^* . This transversality ensures that the degeneracy occurs only at discrete times (i.e., ‘momentarily’ if we may put it like that), and there is actually only one solution to the differential inclusion through (p^A, p^B) . In case (2) there is a unique choice of best responses on Z^* for both players

such that the flow defined by equation (2.2) remains within Z^* . Nearby solutions remain close to and spiral (locally) towards this solution, and so it is the continuous extension of the (unique) flow off Z^* . Again, the apparent non-uniqueness is an artifact; we may say if we like that any attempt to depart from this solution in Z^* is immediately thwarted by the neighbouring flow. Only in case (3) do we find genuine non-uniqueness of solutions to the differential inclusion. This amounts to the fact that there is a choice of best response for each player which keeps the flow within Z^* , and all other choices move you immediately off Z^* in one of two directions. Thus through (p^A, p^B) there are an uncountable set of solutions; one of these remains in Z^* for all time (at least locally), and the others stay in Z^* for some (small) finite time which can be chosen freely, and then fall off in one of the two directions (again chosen freely). From now on we will have little more to say about this, partly because this situation does not arise in the parameter range of most interest to us in our example, but partly also because from a dynamical systems point of view it makes sense to treat these parts of Z^* just as points of discontinuity in a flow which is otherwise uniquely determined.¹³

As mentioned, we do not in this paper consider in any detail the general behaviour near points in Z^* of higher codimension than two. One implication of our results in this paper is that this would be extremely complicated; for example, all the behaviour of the Shapley family studied in this paper can occur in a neighbourhood of points where both players are indifferent between 3 strategies (that is after all one way of thinking of the family).

3 Existence and stability of periodic orbits in the Shapley family

From now we shall concentrate on a particular family example which includes a classical example by Shapley. These examples are given by matrices

$$A = \begin{pmatrix} 1 & 0 & \beta \\ \beta & 1 & 0 \\ 0 & \beta & 1 \end{pmatrix} \quad B = \begin{pmatrix} -\beta & 1 & 0 \\ 0 & -\beta & 1 \\ 1 & 0 & -\beta \end{pmatrix}, \quad (3.7)$$

When $\beta = 0$, this means that the utility of player A is equal to p^B , so player A 's will aim for the largest component of p^B , while player B utility is $(p_3^A, p_2^A, p_1^A) = p^A B$ so is aiming one ahead from the largest component of p^A . So for $\beta = 0$, it is like the paper, scissor, rock game. Our interest is to understand how the behaviour in this game changes when β changes. In Subsection 3.5 we show that the player's actions will become extremely erratic for certain values of β .

Figure 4 shows pictures of the phase space in the cases $-1 < \beta < 0$ and $0 < \beta < 1$, marking the lines where the players are indifferent by dashed lines. (In Figure 1 the phase space was drawn for $\beta = 0$.) Note that for all values of β both players are indifferent between all three strategies at the point $E = (E^A, E^B)$ where $E^A = (E^B)^T = (1/3, 1/3, 1/3)$. Note that when $\beta \neq 0$, for each $p^A \in Z_{ij}^B \subset \Sigma_A$, each aim vector $p^A P_k^A$ is transversal to Z_{ij}^B , and similarly for $p^B \in Z_{ij}^A \subset \Sigma^B$. So the transversality condition of 2.5 holds for $\beta \neq 0$.

¹³Such points may have pre-images in the continuous part of the flow, but this also causes no particular difficulty.

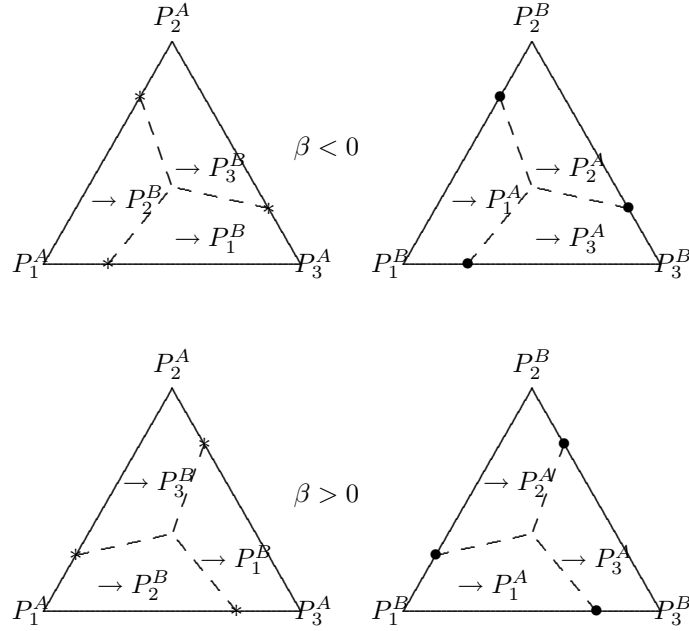


Figure 4: The simplices Σ_A and Σ_B for $\beta < 0$ (above) and $\beta > 0$ (below). For $\beta \in [-1, 1]$, the sets where Player A is indifferent between two strategies are line segments Z_{ij}^A in Σ_B connecting the equilibrium point $E^A = (1/3, 1/3, 1/3)$ to the points $\frac{1}{(2-\beta)}(1, 1-\beta, 0)$, $\frac{1}{(2-\beta)}(1-\beta, 0, 1)$ and $\frac{1}{(2-\beta)}(0, 1, 1-\beta)$ (marked with \bullet). Player B is indifferent between two strategies along line segments Z_{ij}^B in Σ_A connecting the midpoint $(1/3, 1/3, 1/3)$ to the points $\frac{1}{(2+\beta)}(1+\beta, 1, 0)$, $\frac{1}{(2+\beta)}(1, 0, 1+\beta)$ and $\frac{1}{(2+\beta)}(0, 1+\beta, 1)$ (marked with $*$). For $\beta = 0$ these points lie on the middle of the sides of the triangles $\partial\Sigma_A$ and $\partial\Sigma_B$ (as in Figure 1). Increasing $\beta \in [-1, 1]$ rotates the lines anticlockwise (so the end point moves for example from P_2^B towards P_1^B). Note that these indifference lines in the simplices Σ_A and Σ_B do not coincide (despite the appearance of the figure); for example, when $\beta = 1$ then in Σ_B the indifference lines $Z_{i,j}^A$ go through the corners, but the lines $Z_{i,j}^B$ in Σ_A do not.

3.1 Continuity and uniqueness of the flow

We now apply the results of the previous section to the family of examples defined by matrices (3.7). An essential difference between the cases $\beta < 0$ and $\beta > 0$ can be understood in terms of that analysis.

Proposition 3.1 (Continuity and uniqueness). *When $\beta \in (0, 1]$ the unique flow on the complement of the indifference set Z extends to a flow on Z which is everywhere continuous and unique except at $E = (E^A, E^B)$. When $\beta \leq 0$, the unique flow on the complement of Z does not extend continuously to some codimension two surfaces in Z^* . In more detail:*

- If $\beta < 0$ then the transversality condition from Proposition 2.1 holds for all codimension one indifference points in Z . All the codimension two points in Z^* are in cases (1) or

(3), and the flow off Z extends continuously to those points that are in case (1). The differential inclusion (2.2) defines a flow that is unique except at those points, where the flow is discontinuous.

- If $\beta = 0$ then the transversality condition from Proposition 2.1 fails to hold in several codimension-one sets (for example, the set $Z_{1,2}^B \times \{z \in \Sigma_B ; BR_A(p^B) = P_1^A\}$).
- If $\beta > 0$ then the transversality condition from Proposition 2.1 holds on all codimension one indifference sets, and all the codimension two points in Z^* are in case (1) or (2). In particular, the flow off Z extends continuously to all points except $E = (E^A, E^B)$, and so the differential inclusion (2.2) defines a unique and continuous flow everywhere except at the interior equilibrium E .

Proof. This can be seen just by looking at the possible 2×2 games that can be obtained from submatrices of A and B and applying the results from the previous section. (It is also possible to convince oneself of the result graphically by comparing the disposition of lines $Z_{i,j}^{A/B}$ and points P_i^A and P_j^B in Figure 1 and 4.) When $\beta < 0$ case (3) holds, for example, in $Z_{1,2}^B \times Z_{2,3}^A$. When $\beta > 0$ there are points in Z^* , for example on the set $Z_{1,2}^B \times Z_{1,2}^A$ where case (2) arises and trajectories locally spiral around and tend towards Z^* (until they meet another set in Z^*). On the other hand orbits cross $Z_{1,2}^B \times Z_{2,3}^A$ (which is in case (1) transversally when $\beta > 0$). \square

We will see later that when $\beta > 0$ there is genuine non-uniqueness of the flow at E . The spiralling behaviour that can occur near Z^* for $\beta > 0$ contributes significantly to the extra richness of behaviour in $\beta > 0$. The subset $J \subset Z^*$ ¹⁴ on which we have this behaviour consists of the six pieces of Z^* :

$$J = (Z_{1,2}^B \times Z_{3,1}^A) \cup (Z_{1,2}^B \times Z_{1,2}^A) \cup (Z_{2,3}^B \times Z_{1,2}^A) \cup (Z_{1,2}^B \times Z_{2,3}^A) \cup (Z_{3,1}^B \times Z_{2,3}^A) \cup (Z_{2,3}^B \times Z_{3,1}^A) \quad (3.8)$$

The set consisting of the remaining three pieces of Z^* :

$$T = (Z_{1,2}^B \times Z_{2,3}^A) \cup (Z_{2,3}^B \times Z_{3,1}^A) \cup (Z_{3,1}^B \times Z_{1,2}^A) \quad (3.9)$$

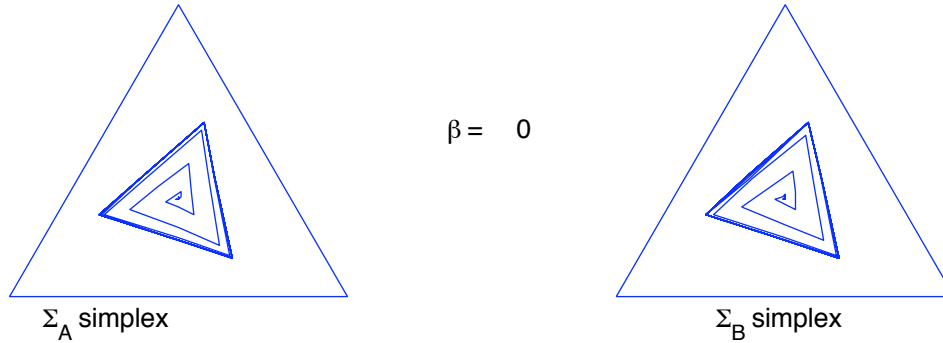
contains the codimension two points where the flow is transversal (case (1)).

3.2 Existence and stability of a clockwise Shapley periodic orbit for $\beta \in (-1, \sigma)$

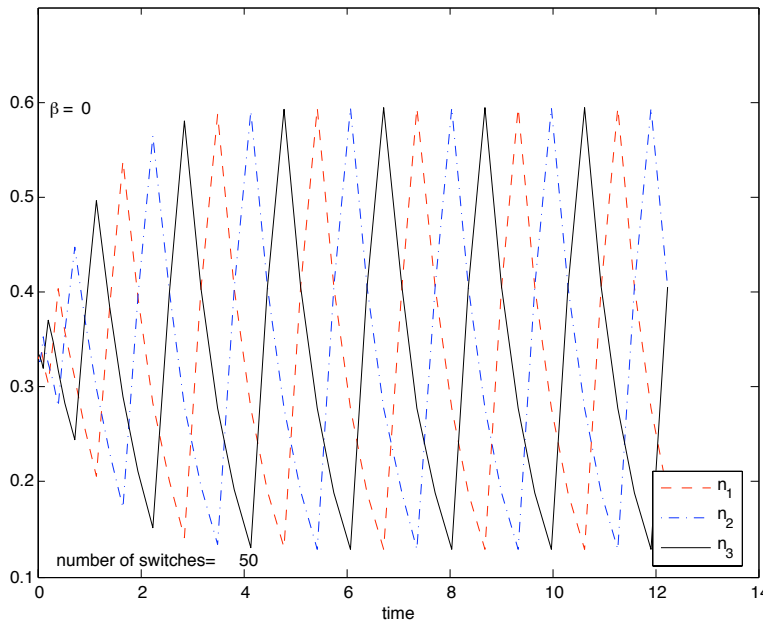
Let σ be the golden mean. We shall first show the existence of a stable periodic orbit for $\beta \in (-1, \sigma)$. We call this the Shapley orbit, as it is the continuation of the orbit described by Shapley [1964] for the case $\beta = 0$, or the clockwise orbit, as the projections of the orbit into the spaces Σ_A and Σ_B rotate clockwise about the equilibrium, see the figure below. In the next subsection we shall also show that this orbit is globally attracting when $\beta \leq 0$. For $\beta = 0$ orbits

¹⁴We could take J to stand for "jitter", since as nearby trajectories spiral around J , both players jitter back and forth between strategies.

spiral away from the equilibrium points towards a periodic orbit (which consists in 4 dimensional phase space $\Sigma_A \times \Sigma_b$ of 6 pieces of straight lines).



The figure below shows the utility $n = Ap^B$ of player A as a function of time for $\beta = 0$. The players move away (in an oscillatory fashion) from the equilibrium point and tend to a periodic motion. Note that where two graphs meet, the players are indifferent between two strategies.



Theorem 3.1 (Existence of the Shapley periodic orbit). For $\beta \in (-1, \sigma)$ there exists a periodic orbit in which player 1 and 2 infinitely repeat the strategies

time	1	2	3	4	5	6
strategy player A	1	2	2	3	3	1
strategy player B	2	2	3	3	1	1

(So player A copies B and player B tries to play one ahead of A.) This is a continuous deformation of the orbit that Shapley found for $\beta = 0$, and as $\beta \uparrow \sigma$ this orbit shrinks in diameter to zero and tends to the point (E^A, E^B) . For $\beta \in (\sigma, 1)$ this periodic orbit no longer exists.

The proof of this Theorem is given in Section 6.1 (in the Appendix). Figure 5 (and later figures up to Figure 7) allow us to illustrate schematically the relationship between regions S_{ij} where player A prefers strategy i and Player B prefers strategy j , $1 \leq i, j \leq 3$. The 9 squares in these diagrams each represent one such region, as labelled. We think of the 3×3 checker board as a torus, so that the top and bottom are identified, as are the left and right sides (so if we go for a walk on the checkerboard and wander off the top, we return with the same horizontal coordinate at the bottom, and similarly if we wander off the left of the diagram we return with the same vertical coordinate on the right). With this convention, the diagram illustrates the adjacency of regions; if just one player changes her preferred strategy, we cross a horizontal or vertical line (representing a codimension-one set) to get to the new region. If we wish both players to change their preferred strategies at the same instant, we must cross diagonally through a corner (representing a codimension-two set) into a new region. Higher codimension points, such as the internal equilibrium (E^A, E^B) where all regions meet, are not represented. Note also that each region is actually 4-dimensional, rather than 2 as represented in the diagram, and so if we wish to project trajectories of the system onto the diagram we may find that they cross; certainly we do not want to claim there is any sort of unique flow determined on the checkerboard.

The usefulness of these diagrams is that we may add arrows showing which transitions are allowed, which we will use in the proof of the theorem. Thus, for example, if we imagine that we begin in the top left-hand region where $A \rightarrow P_1^A$ and $B \rightarrow P_2^B$ then inspection of Figure 1 for $\beta = 0$ shows that the only region we can move to (and indeed will move to in due course) is the region where $A \rightarrow P_2^A$ and $B \rightarrow P_2^B$, as represented by the arrow between these two regions in Figure 5. The other arrows are computed similarly. In regions such as $A \rightarrow P_1^A$ and $B \rightarrow P_3^B$ there is a codimension-one set such that trajectories started on this set will reach indifference lines in Σ_A and Σ_B simultaneously. This set is represented by the dotted line in the appropriate square in Figure 5, and similarly in other squares where this occurs. Finally, some of the codimension one indifference surfaces are represented by dashed lines in the $\beta = 0$ case. This is rather special, and is where the transversality condition of Proposition 2.1 fails; orbits move off in different directions on opposite sides of these lines. Figure 6 for $\beta < 0$ is rather similar, and the extra dotted lines are explained in the caption.

Let us call the discontinuity set the subset of Z^* for which type (1) behaviour occurs. It has (of course) measure zero.

Theorem 3.2 (The Shapley orbit is globally attracting for $\beta \leq 0$). *For $\beta \leq 0$, the flow has a unique closed orbit (the Shapley orbit); the flow of all initial conditions which do not enter the discontinuity set tends to this closed orbit.*

Proof. When $\beta \leq 0$, then the only regions which can be entered are those marked with a central integer label. So any trajectory which does not enter the discontinuity set, eventually enters one of these regions. (These orbits form a set of zero Lebesgue measure.) From the diagram it is clear that from then on the orbit cyclically visits the regions 1-6. Now consider, for example, the part S_1 of the space $Z_{1,2}^A$ where player A is indifferent between strategies P_2^A and P_1^A , and player B strictly prefers strategy P_2^B (this corresponds in the diagram to the line dividing regions labelled 1 and 2). Similarly consider the region S_2 where the orbits leave region labelled 2. Each of these sets S_i is the product of a line segment and a kite-shaped quadrangle, with one boundary point the equilibrium point E . Now consider the map T which assigns to a point in S_1 the first visit of the forward orbit through x to S_2 . Since all orbits in region 1 will aim for the same point and only exit via S_2 (when $\beta \in (-1, 0]$), this map is continuous; moreover, for each $(p^A, p^B) \in S_1$ we

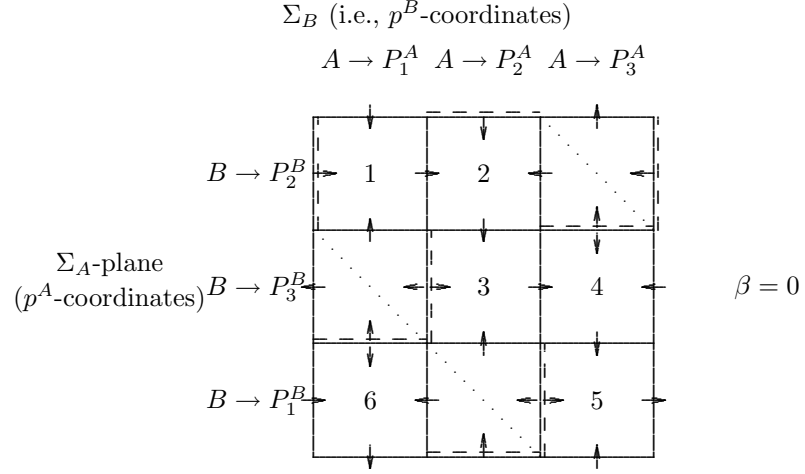


Figure 5: A diagram showing allowed transitions between regions of pure preference for $\beta = 0$. See the text for explanations of dotted and dashed lines.

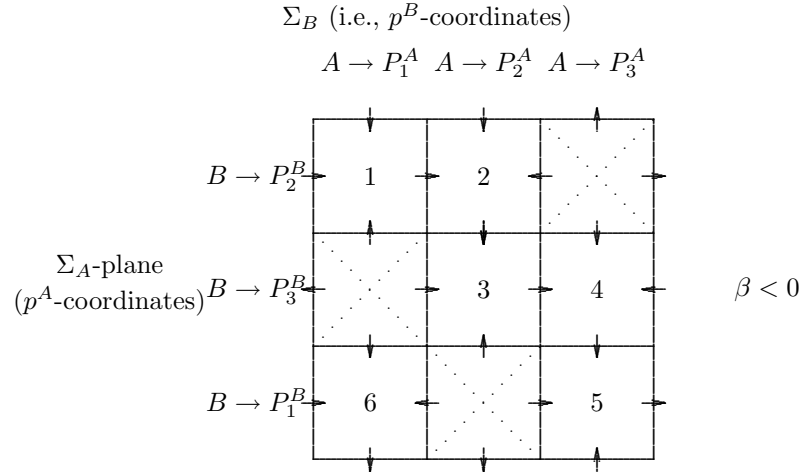


Figure 6: The transition diagram of the flow for $\beta < 0$. The dotted lines again indicate the codimension-one sets where p^A and p^B leave the relevant regions simultaneously. The points where these dotted lines meet, correspond to a set of initial conditions where the trajectory exits the region by hitting $E^A = E^B = (1/3, 1/3, 1/3)$.

have $T(p^A, p^B)$ except when $p^A = E^A$. In fact, T a central projection. In other words, if we put linear coordinates on S_1 and S_2 then $T: S_1 \rightarrow S_2$ takes the form

$$T(z) = \frac{1}{f(z)}L(z) \tag{3.10}$$

where $L: S_1 \rightarrow S_2$ and $f: S_1 \rightarrow \mathbb{R}$ are affine transformations. So in linear coordinates,

$$T(x, y, z) = \left(\frac{a_1 + b_1x + c_1y + d_1z}{a + bx + cy + dz}, \frac{a_2 + b_2x + c_2y + d_2z}{a + bx + cy + dz}, \frac{a_3 + b_3x + c_3y + d_3z}{a + bx + cy + dz} \right).$$

(These maps are explicitly calculated in the appendix; here we shall only use that it is of this form.) Note that compositions of such maps are again of this form. If

$$T_1 = \frac{1}{f_1}L_1 \text{ and } T_2 = \frac{1}{f_2}L_2$$

are two such transformations and we take linear coordinates such that $T_1(0) = 0$ (i.e. $L_1(0) = 0$) then the composition formula becomes particularly simple:

$$T_2 \circ T_1 = \frac{1}{f_2(T_1(z)) \cdot f_1(z)} L_2 \circ L_1(z). \quad (3.11)$$

Note that because of cancellations $f_2(T_1(z)) \cdot f_1(z)$ actually is an affine map in z .

Now let P be the first return map to S_1 . As we observed P is a continuous central projection as above, so of the form $z \mapsto P(z) = \frac{1}{f(z)}L(z)$ with $P(S_1) \subset S_1$ and

$$P(S_1) \subset \text{interior}(S_1) \cap E \quad (3.12)$$

P has a fixed p in the interior of S_1 corresponding to the Shapley periodic orbit. Let us show that $\lim_{n \rightarrow \infty} P^n(x) \rightarrow p$ for each $x \in S_1 \setminus E$, where P^n is the n -th iterate of P . To see this, notice that P sends lines to lines and restricted to each line, T is a Moebius transformation, i.e. of the form $t \mapsto \frac{\alpha + t\beta}{\gamma + t\delta}$ (where we take affine coordinates on the lines). Let us first consider the line l_0 through p and E , and let b be so that $l_0 \cap S_1 = [E, b]$. This line l_0 is mapped into itself because $p, E \in l_0$ are both fixed points. $P: l_0 \rightarrow l_0$ is a Moebius transformation which sends the line segment $[E, b] = l_0 \cap S_1$ continuously into $[a, b]$ (this is because of (3.12)) and having fixed point $p \in (E, b)$. It follows from this that for any $x \in (E, b]$, $\lim_{n \rightarrow \infty} P^n(x) \rightarrow p$. Now consider any other eigendirection l through x . Because of (3.12), P maps $l \cap S_1$ continuously strictly inside itself, and since the restriction of P to this line is a Moebius transformation, again all points in $l \cap S_1$ converge to p . If P has a complex eigenvalue then the argument is similar.

To consider any other point x , take the projective space \mathbb{P} of lines through p in S_1 . The return map P assigns to each line $\hat{x} \in \mathbb{P}$ a new line $\hat{P}(\hat{x}) \in \mathbb{P}$. The eigenvalues of the linear transformation L correspond to fixed points of \hat{P} , and for each line l through x in S_1 , $P^n(l)$ tends to an eigenspace of the linearisation of P at x . Combining this with the above, it follows that for each $x \in S_1 \setminus E$, $P^n(x) \rightarrow p$.

It follows that for the original flow all trajectories which do not enter the discontinuity set are attracted to the periodic Shapley orbit. \square

This theorem completes our investigation of $\beta \leq 0$.

3.3 Existence and Stability of an Shapley and also an anti-Shapley periodic orbit for $\beta > 0$

Let us now consider orbits when $\beta \in (0, 1]$. The transition diagram for this case is given in Figure 7 and it is immediately clear that there are now many more possible routes that may

be taken from region to region. We stress that the existence of a possible route allowed by the arrows, does not necessarily imply the existence of a corresponding trajectory in the flow; we will need to perform some calculations to see which routes are actually realised for any given value of β . In this figure the dashed lines represent codimension-one sets of points from which trajectories tend, for one or other player, to E^A or E^B . The sequence of regions visited will be different depending which side of these sets you begin. [We should note that the dashed curves do not move entirely across the squares as $\beta \rightarrow 1$ (because the points in Figure 4 marked with \bullet in Σ_B still have not reached the corners of Σ_B when $\beta = 1$).]

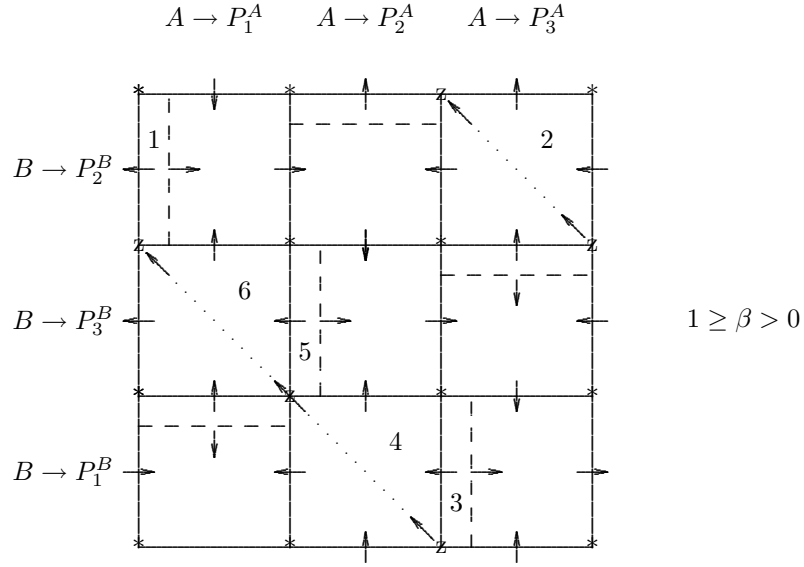


Figure 7: The transition diagram of the flow for $\beta \in (0, 1]$. Boxes again represent regions S_{ij} , and arrows indicate possible transitions between regions. Routes may now spiral around near the ‘corners’ marked with $*$; these 6 corners represent codimension-two points on the six pieces of J . The 3 corners marked z represent codimension-two points on the 3 pieces of $Z^* \setminus J$ and trajectories cross these sets transversally; there is no spiralling. The numbers 1 – 6 in the regions show a possible route for an anticlockwise periodic orbit. Notice that the route for the clockwise Shapley orbit is still also allowed. The dashed lines correspond to preimages of points (E^A, p^B) or (p^A, E^B) , whereas the dotted lines correspond to preimages of $Z^* \setminus J$, but where the orbits will cross transversally as in case (1) above. When $\beta = 1$ the situation remains almost the same except that it is no longer possible to have two types of exits from the regions with the dotted lines (no exit is possible in the horizontal direction in the three relevant boxes, but this restriction does not prevent the continued existence of the anticlockwise route marked).

We show in the Appendix, by direct calculation, that precisely one of the anticlockwise or clockwise orbits mentioned in the figure caption exists when $\beta \neq \sigma$, where $\sigma = (-1 + \sqrt{5})/2$, the golden mean. In particular, for $\beta \in [-1, \sigma)$ there is an attracting orbit which goes round the midpoint of Σ_A and Σ_B in a clockwise fashion (this is a continuous deformation of Shapley’s periodic orbit for $\beta = 0$, which we have already studied in the previous section for $\beta \leq 0$), whereas for $\beta \in (\sigma, 1]$ there is a different periodic orbit which goes around these points in a anticlockwise fashion. It is attracting for some interval of β values to be described further below,

and is otherwise of saddle-type.

Theorem 3.3 (Existence and stability of the Shapley and anti-Shapley periodic orbits). *For $\beta \in [0, \sigma)$ there exists the periodic orbit mentioned already in Theorem 3.1, i.e. it visits, in the same order, the same regions as the Shapley orbit of Theorem 3.2. This is a continuous deformation of that orbit, and as $\beta \uparrow \sigma$ this orbit shrinks in diameter to zero and tends to the point (E^A, E^B) . This orbit is stable for all $\beta \in [0, \sigma)$.*

For $\beta \in (\sigma, 1]$ there exists a periodic orbit (anticlockwise) which visits the regions marked 1-6 in Figure 7 cyclically in order, i.e., follow the following pattern:

<i>time</i>	1	2	3	4	5	6
<i>strategy player A</i>	1	1	3	3	2	2
<i>strategy player B</i>	3	2	2	1	1	3

As $\beta \downarrow \sigma$ this orbit shrinks in diameter to zero and tends to the point (E^A, E^B) . Such a periodic orbit does NOT exist when $\beta < \sigma$.

Shapley's (clockwise) periodic orbit is attracting for all $\beta \in [0, \sigma)$. The anti-Shapley (anticlockwise) periodic orbit which exists for $\beta \in (\sigma, 1]$ is attracting when $\beta \in (\tau, 1)$ and of saddle-type when $\beta \in (\sigma, \tau)$. Here τ is the root of some specific expression and is approximately 0.915.

We remark that it does not seem to be possible to prove the existence of the anticlockwise orbit, even when $\beta = 1$, by the same sort of technique as we used to prove the existence of the clockwise orbit in $\beta \leq 0$. This is because even when $\beta = 1$ the relevant version of Figure 7 still allows many routes through the diagram; it was only because there was only a single route possible in the $\beta \leq 0$ case that we were able to deduce that an orbit following that route must exist. Neither the Shapley nor the anti-Shapley orbits attract every starting position: as we show in the sequel to this paper [2006], there are an uncountable number of orbits which tend to the interior equilibrium point. The existence of one such orbit is shown in the next subsection.

The proof of this Theorem is in the Appendix, as is a discussion of the bifurcation at $\beta = \tau$.

3.4 Dynamics and a periodic orbit Γ on the set J

We will now consider the flow on the set J (more precisely, the unique continuous extension of the flow to J). The dynamics near J is very interesting because orbits can spiral for very long periods near J near this orbit, before moving away. Because on J at least one of the two players is indifferent between two strategies, nearby orbits correspond to behaviour where players frequently switch their preferred behaviour.

We shall prove here that trajectories on J visit the six pieces cyclically (in the order in which they appear in the definition in equation (3.8)), and the details of the behaviour are given in the following proposition (see Figure 8).

Theorem 3.4 (A third periodic which is created by a Hopf-like bifurcation). *The system has a Hopf-like bifurcation when $\beta = \sigma$ on the topological two-dimensional manifold J . Trajectories on J spiral towards (E^A, E^B) when $\beta \in (0, \sigma]$ while for $\beta \in (\sigma, 1]$ all trajectories in J (except the one stationary at (E^A, E^B)) tend to a periodic orbit Γ in J .*

We denote the endpoints of Γ along the pieces of J by f_{ij}^A and f_{kl}^B , as in Figure 8. Then for $\beta \in (\sigma, 1)$ one has the following formulas for the ‘diameter’ of the periodic orbit Γ :

$$\frac{|E_{kl}^B - f_{kl}^B|}{|Q_{kl}^B - f_{kl}^B|} = \frac{|f_{ij}^A - m_{ij}^A|}{|R_{ij}^A - E_{ij}^A|} = \frac{\beta^2 + \beta - 1}{2\beta + 1}$$

and

$$\frac{|f_{kl}^B - E_{kl}^B|}{|R_{kl}^B - E_{kl}^B|} = \frac{|E_{ij}^A - f_{ij}^A|}{|Q_{ij}^A - f_{ij}^A|} = \frac{\beta^2 + \beta - 1}{(1 + \beta)^2}.$$

Note that these expressions are both increasing in $\beta \in (\sigma, 1]$ and are zero when $\beta = \sigma$ (but unlike the usual Hopf-bifurcation the diameter increases roughly linearly when $\beta - \sigma > 0$ is small). They achieve their maximum $1/3, 1/4$ both at $\beta = 1$.

The proof of this Theorem is a tedious calculation and can be found in the appendix. Note that it is also argued there that trajectories spiralling into (E^A, E^B) on J for $\beta < \sigma$, or out of it for $\beta > \sigma$, do so in finite time. There is genuine non-uniqueness of the flow at (E^A, E^B) reflecting the fact that it is the only point (for $\beta > 0$) at which we cannot continuously extend the flow.

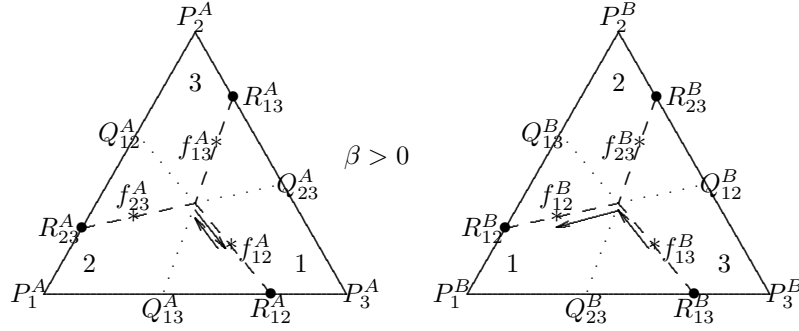
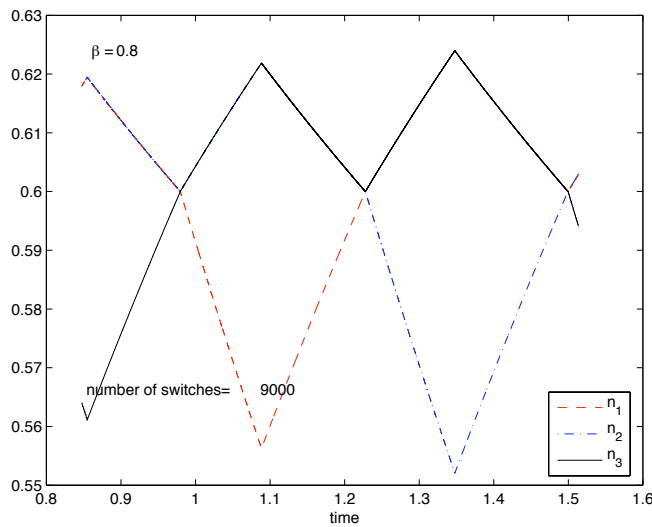
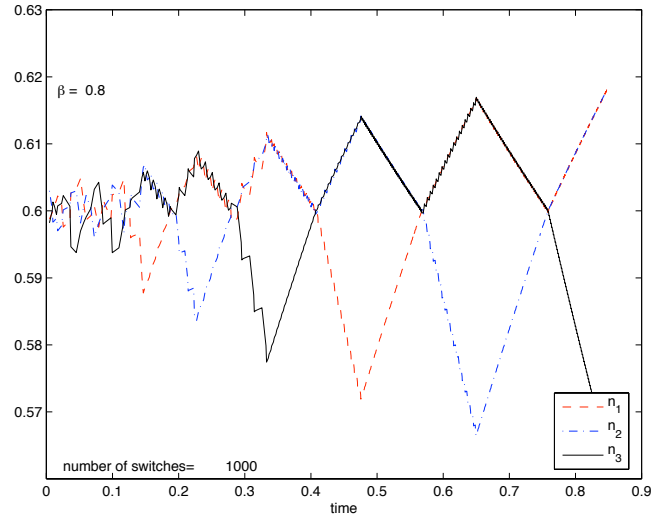


Figure 8: The simplices Σ_A and Σ_B . Various points on the sets Z^A and Z^B (and their extensions) are drawn. $R_{23}^A = \frac{1}{2+\beta}(1 + \beta, 1, 0)$, $Q_{12}^A = \frac{1}{1+2\beta}(\beta, 1 + \beta, 0)$ (and similarly formulas for the other points by cyclically permuting coordinates). Similarly $R_{12}^B = \frac{1}{2-\beta}(1, 1 - \beta, 0)$ and $Q_{13}^B = \frac{1}{1+\beta}(\beta, 1, 0)$. The points f_{ij}^A, f_{kl}^B give the maximum extent of the periodic orbit on J ($\beta > \sigma$ only). Take $(p^A, p^B) \in (Z_{1,2}^B \times Z_{3,1}^A)$ as starting points. Then $p^A(t)$ moves along $Z_{1,2}^B$ towards R_{12}^A and $p^B(t)$ moves towards the midpoint of Σ_B along $Z_{1,3}^A$. Once $p^B(t)$ hits the midpoint of Σ_B (provided $p^A(t) \neq (1/3, 1/3, 1/3)$) then the flow extends continuously and $(p^A(t), p^B(t))$ enters $Z_{1,2}^B \times Z_{1,2}^A$. Along this set $p^A(t)$ then moves back along $Z_{1,2}^B$ towards the midpoint in Σ_A while $p^B(t)$ moves towards R_{12}^B . Next it enters the third part of J , and in this way the orbit spirals (cyclically) around the different legs of J .

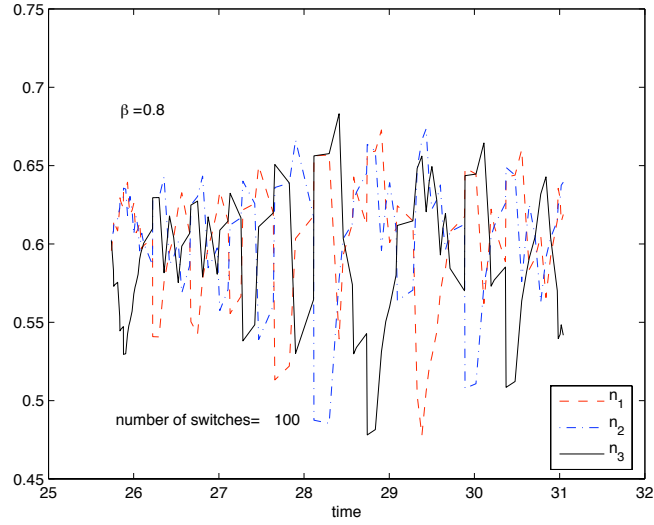
3.5 Dithering and chaotic behaviour near J

It is not true that this orbit is attracting for orbits that start off J . Nonetheless, orbits of the system for $\beta > \sigma$ can spend long times near to this orbit J . The reason for this is that orbits can

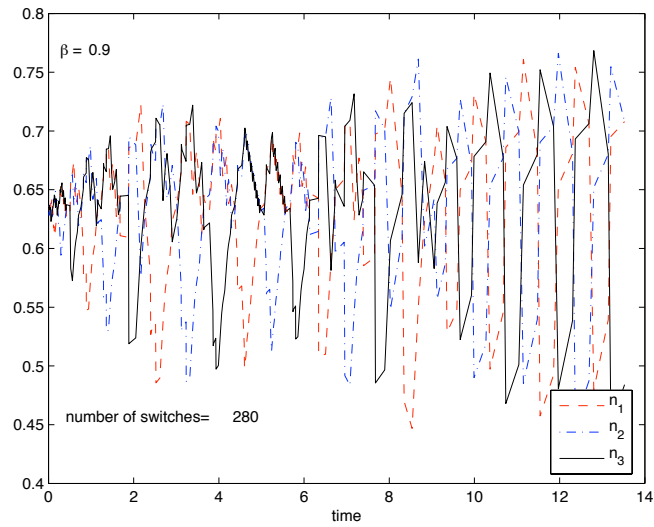
spiral along cones whose axes consist of the 6 legs of the periodic orbit on J in the way described in Figure 3. The next two figure below shows a portion of a numerically computed trajectory for $\beta = 0.8$. The orbit shown, starts near the centre, and during the time interval considered comes close to the periodic orbit J , while jittering a large number of times near this orbit. Notice that the short time intervals and the large number of time the players switch strategies.

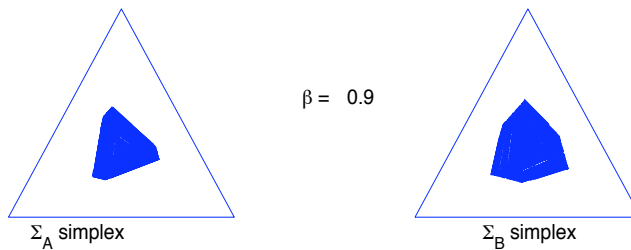


The same orbit shown for a later time interval, shows that orbits eventually become less periodic.



In fact, as will be made precise in [2006], one has chaotic motion for $\beta \in [\sigma, \tau]$. The figures below show orbits for $\beta = 0.9$, both showing erratic time-series and the attracting set projected on Σ^A and Σ^B .





4 Conclusion

For $\beta \in (-1, 0]$ players always asymptotically become periodic. When $\beta \in (0, \sigma)$ the Shapley orbit is still attracting but not globally attracting: there are orbits as described in Theorem 3.4 which tend to E . In a sequel to this paper we shall show that there infinitely many such cone-like sets consisting of points which tend to E . (So the stable manifold of E is extremely complicated.)

The numerical results showed that for $\beta \in (\sigma, \tau)$ players act erratically and chaotically. In the sequel to this paper we shall give rigorous results which explain this behaviour. The mathematical methodology in this sequel paper will be more geometric (and will be based on first projecting the flow on a three-sphere and then by a study of the first return dynamics to a global two-dimensional section consisting of a disc bounded by the periodic orbit Γ).

Finally, when $\beta \in (\tau, 1)$ orbits tend to a so-called anti-Shapley orbit.

Of course most of the analysis we described also could be applied to other families (with less symmetry). We will go into this in the sequel to this paper. Finally, simulations and preliminary theoretical considerations indicate that for $n \times n$ games with $n > 3$ there are other routes to chaotic behaviour than those studied here.

5 Bibliography

References

- [2003] Berger, U. (2003). Two More Classes of Games with the Continuous-time Fictitious Play Property. Vienna University Department of Economics and Business Administration Discussion Paper.
- [2005] Berger, U. (2005): “Fictitious play in $2 \times n$ games, *Journal of Economic Theory*, 120, 139-154.
- [1949] Brown, G. W. (1949): “Some Notes on Computation of Games Solutions”, The Rand Corporation, P-78, April.
- [1951a] Brown, G. W. (1951a): “Iterative Solutions of Games by Fictitious Play”, in T. C. Koopmans, ed., “Activity Analysis of Production and Allocation”, John Wiley & Sons, New York, 374-376.
- [1951b] Brown, G. W. (1951b): “Notes on the Solution of Linear Systems Involving Inequalities”, in “Proceedings of a Second Symposium on Large Scale Digital Calculating Machinery”, The Annals of the Computation Laboratory of Harvard University, 26, Harvard University Press, Cambridge, Massachusetts, 137-140.
- [1992] Cowan, S.G. (1992): “Dynamical Systems arising from Game Theory”, Ph D thesis, University of California at Berkeley.
- [1998] Ellison, G. and Fudenberg, D. (1998): “Learning Purified Mixed Equilibria”, mimeo, Massachusetts Institute of Technology.
- [1993] Fudenberg, D. and Kreps, D. (1993): “Learning Mixed Equilibria”, *Games and Economic Behavior*, 5, 320-367.
- [1995] Fudenberg, D. and Levine, D. (1995): “Consistency and Cautious Fictitious Play”, *Journal of Economic Dynamics and Control*, 19, 1065-1090.
- [1998] Fudenberg, D. and Levine, D. (1998): “The Theory of Learning in Games”, MIT Press.
- [1995] Gaunersdorfer, A. and Hofbauer, J. (1995): “Fictitious play, Shapley polygons, and the replicator equation” *Games and Economic Behavior* 11, 279-303.
- [1983] Guckenheimer, J. and Holmes, Ph. (1983): “Nonlinear oscillations, dynamical systems, and bifurcations of vector fields”, *App. Math. Sc* **42**, Springer Verlag.
- [1999] Hahn, S. (1999): “The convergence of Fictitious Play in 3×3 games with strategic complementarities”. *Economics Letters* 64, 57-60.
- [1998] Harris, C. (1998): “On the Rate of Convergence of Fictitious Play”, *Games and Economic Behavior*, 22, 238-259.
- [1995] Hofbauer, J. (1995). “Stability for the best response dynamics”. Mimeo, University of Vienna.

- [1993] Jordan, J. S. (1993). Three problems in learning mixed-strategy Nash equilibria. *Games and Economic Behavior* 5, 368-386.
- [1992] Krishna, V. (1992). “Learning in games with strategic complementarities”. Mimeo, Harvard University.
- [1994] Metrick, A. and Polak, B. (1994): “Fictitious Play in 2×2 Games: a Geometric Proof of Convergence”, *Economic Theory*, 4, 923-933.
- [1991] Milgrom, P. and Roberts, J. (1991). Adaptive and sophisticated learning in normal form games. *Games and Economic Behavior* 3, 82-100.
- [1961] Miyasawa, K. (1961): “On the Convergence of the Learning Process in a 2×2 Non-Zero-Sum Two-Person Game”, Economic Research Program, Princeton University, Research Memorandum No. 33.
- [1996] Monderer, D., and Shapley, L. S. (1996a): “Fictitious-Play Property for Games with Identical Interests”, *Journal of Economic Theory*, 68, 258-265.
- [1951] Robinson, J. (1951): “An Iterative Method of Solving a Game”, *Annals of Mathematics*, 54, pp. 296-301.
- [1998] Sela, A. (1998): “Fictitious Play in 2×3 Games”, Economics Department, Ben-Gurion University of the Negev.
- [1964] Shapley, L. S. (1964): “Some Topics in Two-Person Games”, in M. Dresher, L. S. Shapley and A. W. Tucker, eds., “Advances in Game Theory”, *Annals of Mathematics Studies* No. 52, 1-28.
- [2006] Sparrow, C. and van Strien, S. (2006), “In preparation”.

6 Appendix

In this appendix we collect together a number of explicit calculations that are used in the main text.

It is convenient to work in the space (v^A, v^B) where $v^A = Ap^B$ and $v^B = p^A B$ (so v^A is a column vector, and v^B is a row vector). From the description of the dynamics in the main text, when v_i^A is the largest coordinate of v^A , player A adjusts p^A towards P_i^A , which implies v^B moves in a straight line towards B_i , the i^{th} row of B . Similarly, if v_j^B is the largest component of v^B , v^A moves towards A_j , the j^{th} column of A . In both cases, our convention is that the motion occurs at a speed such that from a given initial condition, and assuming that i and j were to remain the maximal coordinates of v^A and v^B , the vectors would reach B_i and A_j in one unit of time. So, for $0 \leq s \leq 1$, provided the maximal coordinate of v^A or v^B does not change, we can write

$$\begin{aligned} v^A(t+s) &= v^A(t) + s(A_j - v^A(t)) \\ v^B(t+s) &= v^B(t) + s(B_i - v^B(t)) \end{aligned} \quad (6.13)$$

Each time that the maximal coordinate of either v^A or v^B changes, we reset s in (6.13) to zero. In this appendix we calculate explicit orbits with particular properties, using these equations.

We illustrate our calculations with figures that show the development of the components of v^A and v^B with time. Let $\sigma = (-1 + \sqrt{5})/2$, the golden mean.

6.1 Existence of the clockwise Shapley orbit in $\beta \in (-1, \sigma)$

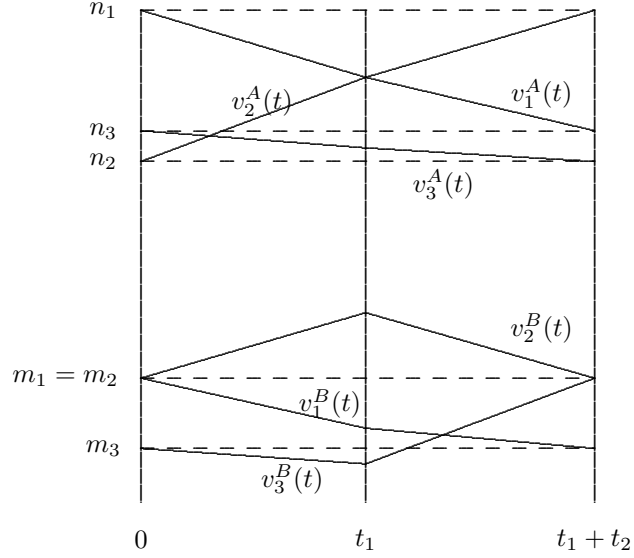


Figure 9: Components of v^A and v^B plotted against time for one third of the symmetric Shapley (clockwise) periodic orbit which exists for $\beta \in [0, \sigma)$. Since v_2^B is maximal throughout, $v^A(t)$ moves towards $A_2 = (0, 1, \beta)^T$. In the interval $[0, t_1]$ coordinate v_1^A is maximal and $v^B(t)$ moves towards $B_1 = (-\beta, 1, 0)$; in the interval $[t_1, t_1 + t_2]$, v_2^A is maximal and $v^B(t)$ moves towards $B_2 = (0, -\beta, 1)$.

Let us compute the clockwise Shapley periodic orbit which, as we will see, exists for $\beta \in (-1, \sigma)$. The periodic orbit we are looking for is rotation symmetric, so we will only compute the part of the orbit where player B prefers strategy 2 (while player A prefers first strategy 1 and then strategy 2); see Figure 9.

Let $n = (n_1, n_2, n_3)^T$ and $m = (m_1, m_2, m_3)$ be the initial values of v^A and v^B respectively. Then we require, as shown in the figure, that

$$n_1 > \max(n_2, n_3) \quad \text{and} \quad m_1 = m_2 > m_3, \quad (6.14)$$

so that initially v^A heads towards $A_2 = (0, 1, \beta)^T$ and v^B towards $(-\beta, 1, 0) = B_1$. The first time t_1 that the orbit meets Z again is when the first and second coordinates of $v^A(t) = (1-t)n^T + t(0, 1, \beta)^T$ become equal which occurs when $t = t_1 > 0$,

$$t_1 = \frac{n_1 - n_2}{n_1 - n_2 + 1}.$$

(Of course, it is possible that we first get that $n_1 = n_3$, but this does not occur because $n_1 = n_3$ happens when $t' = \frac{n_1 - n_3}{n_1 - n_3 + \beta}$ which is larger than t_1 as $\beta < 1$.) The v^A and v^B values at $t = t_1$

are

$$v^A(t_1) = \frac{1}{(n_1 - n_2 + 1)} \begin{pmatrix} n_1 \\ n_2 + (n_1 - n_2) \\ n_3 + (n_1 - n_2)\beta \end{pmatrix}$$

and

$$v^B(t_1) = \frac{1}{(n_1 - n_2 + 1)} (m_1 - \beta(n_1 - n_2), m_2 + (n_1 - n_2), m_3) .$$

Next we have that $t_2 > 0$ is the smallest number so that the second and third coordinate of $v^B(t_1 + t_2) = (1 - t_2)v^B(t_1) + t_2(0, -\beta, 1)$ are equal. This gives

$$t_2 = \frac{m_2(t_1) - m_3(t_1)}{m_2(t_1) - m_3(t_1) + 1 + \beta} = \frac{(m_2 - m_3) + (n_1 - n_2)}{(m_2 - m_3) + (n_1 - n_2) + (1 + \beta)(1 + n_1 - n_2)}$$

which implies

$$v^A(t_1 + t_2) = \frac{1}{X} \begin{pmatrix} n_1(1 + \beta) \\ n_1(1 + \beta) + \delta \\ ((n_3 + (n_1 - n_2)\beta)(1 + \beta) + \beta\delta) \end{pmatrix}, \quad (6.15)$$

and

$$v^B(t_1 + t_2) = \frac{1 + \beta}{X} ((m_1 - \beta(n_1 - n_2)), (m_2 + (n_1 - n_2)) - \beta\delta, m_3 + \delta/(1 + \beta)) \quad (6.16)$$

where $\delta = (m_2 - m_3) + (n_1 - n_2)$ and $X = \delta + (1 + \beta)(1 + n_1 - n_2)$. For a symmetric periodic orbit we have to satisfy

$$v^A(t_1 + t_2) = \begin{pmatrix} n_3 \\ n_1 \\ n_2 \end{pmatrix} \quad \text{and} \quad v^B(t_1 + t_2) = \begin{pmatrix} m_3 \\ m_1 \\ m_1 \end{pmatrix}, \quad (6.17)$$

and the strict inequalities (6.14). Solving equations (6.15)–(6.17) by hand (or by a MAPLE worksheet ¹⁵ gives

$$n_1 = \nu \quad (6.18)$$

$$n_2 = -\frac{-2\beta^2 - \beta^3 + 2\nu\beta^3 - 3\nu\beta - 2\nu + 3\nu^2 + 3\nu^2\beta^2 + 3\nu^2\beta}{1 + \beta + \beta^2}, \quad (6.19)$$

$$n_3 = \frac{2\beta + 1 + 2\nu\beta^3 - \nu\beta^2 - 4\nu\beta - 3\nu + 3\nu^2 + 3\nu^2\beta^2 + 3\nu^2\beta}{1 + \beta + \beta^2}, \quad (6.20)$$

$$m_2 = m_1 = 1 - \nu - \nu\beta \quad (6.21)$$

$$m_3 = -\beta + 2\nu\beta - 1 + 2\nu, \quad (6.22)$$

where ν satisfies $f_\beta(\nu) = 0$ with

$$f_\beta(Z) = (3\beta^2 + 3\beta + 3)Z^3 + (2\beta^3 - 2\beta^2 - 5\beta - 4)Z^2 + (-\beta^3 + 4\beta + 3)Z - 1 - \beta. \quad (6.23)$$

¹⁵which can be downloaded from <http://www.maths.warwick.ac.uk/~strien/Publications>

Note that for $\beta \in (-1, 1)$, $f_\beta(0) = -1 - \beta < 0$ and $f_\beta(1) = \beta^3 + \beta^2 + \beta + 1 > 0$. For $\beta \in (-1, 1)$, the function $t \mapsto f_\beta(t)$ is monotone because its derivative

$$f'_\beta(Z) = 3(3\beta^2 + 3\beta + 3)Z^2 + 2(2\beta^3 - 2\beta^2 - 5\beta - 4)Z + (-\beta^3 + 4\beta + 3) \quad (6.24)$$

is a strictly positive quadratic function; this is because its discriminant is equal to $16\beta^6 + 4\beta^5 - 28\beta^4 - 92\beta^3 - 88\beta^2 - 92\beta - 44$ and so is negative when $\beta \in (-1, 1)$. Hence, for $\beta \in (-1, 1)$ the cubic (6.23) has a unique real root ν , and this root is in $(0, 1)$. Moreover, this solution ν depends continuously on β . When $\beta = 0$, this solution satisfies the inequalities that guarantee the behaviour is as shown in the figure: indeed when $\beta = 0$ then we obtain $n_1 = 0.594\dots$, $n_2 = 0.129\dots$, $n_3 = 0.277\dots$, $m_1 = 0.405\dots$, $m_2 = m_3 = 0.188\dots$

Let us show that equalities can only hold in (6.14) when $\beta \notin (-1, 1)$ or $\beta = \sigma$. If $m_1 = m_3$ then the expressions for m_1 and m_3 give $\nu_\beta = (2 + \beta)/(3 + 3\beta)$ and then

$$f_\beta(\nu_\beta) = -\frac{(\beta^2 + \beta - 1)(1 + \beta + \beta^2)^2}{9(1 + \beta)^3} = 0;$$

this implies that either $\beta \notin (-1, 1)$ or β is equal to the golden mean σ . If $n_1 = n_3$ then because of the first equation in (6.17) the first two components $v^A(t_1 + t_2)$ in (6.15) are equal, and so $\delta = 0$; using these two equation again we get $n_1 - n_2 = 0$ and with $\delta = 0$ this implies $m_1 = m_3$ and therefore as we saw $\beta \notin (-1, 1)$ or $\beta = \sigma$. If $n_1 = n_2$ then $X = \delta + 1 + \beta$ and

$$v^A(t_1 + t_2) = \frac{1}{X} \begin{pmatrix} n_1(1 + \beta) \\ n_1(1 + \beta) + \delta \\ n_3(1 + \beta) + \beta\delta \end{pmatrix} = \begin{pmatrix} n_3 \\ n_1 \\ n_1 \end{pmatrix}$$

which gives that $\delta n_3 + \delta = \beta\delta$ and so either $\delta = 0$ or $n_3 = \beta - 1$ and so $\nu = n_1 = n_2 = 1$. The latter is impossible because $f_\beta(1) > 0$ while the latter implies that $m_2 = m_3$ (we assumed that $n_1 = n_2$); as we showed above $m_2 = m_3$ implies $\beta \notin (-1, 1)$ or $\beta = \sigma$.

It follows that there exists a symmetric clockwise periodic orbit for all $\beta \in (-1, \sigma)$, depending continuously on β . As $\beta \uparrow \sigma$ this periodic orbit shrinks to the equilibrium solution $n_1 = n_2 = n_3 = (1 + \beta)/3$ and $m_1 = m_2 = m_3 = (1 - \beta)/3$. To see this, notice that $f_\beta((1 + \beta)/3) = 0$ is a fifth order equation which can be factorized as

$$\frac{1}{3}(1 + \beta)(\beta^2 + \beta - 1)(\beta^2 - \beta + 1) = 0$$

which is zero if $\beta = \sigma$ or $\beta \notin (-1, 1)$. If $\beta \in (\sigma, 1)$ the inequalities in (6.14) no longer hold. This can be seen by considering the solutions for $\beta = 1$ in (6.18-6.22).

6.2 Existence of the anticlockwise periodic orbit when $\beta \in (\sigma, 1)$.

We first show that for $\sigma < \beta \leq 1$ there exists a unique symmetric anticlockwise periodic orbit as described in Theorem 3.3 in the main text.

For such an orbit to exist, with the appropriate symmetry, the vectors v^A and v^B must behave as shown in Figure 10 below.

We compute only the part of the orbit where player B prefers strategy 2, starting where player B is indifferent between strategies 2 and 3, and ending where player B is indifferent between

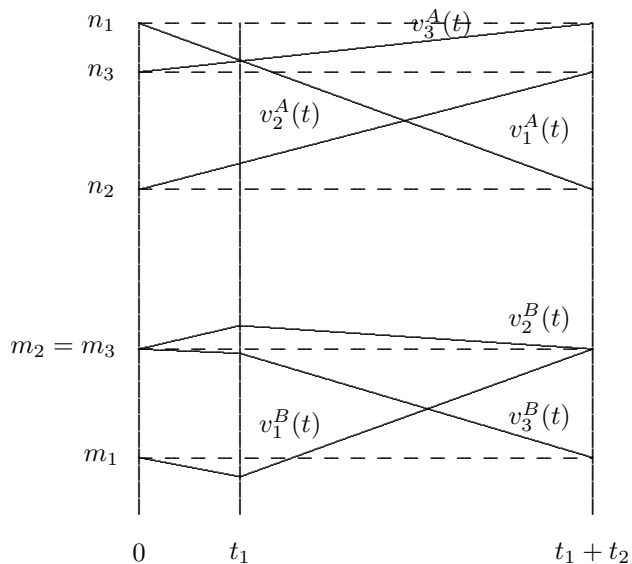


Figure 10: Components of v^A and v^B plotted against time for one third of the symmetric (anticlockwise) periodic orbit which exists for $\beta \in (\sigma, 1]$. Note that the identity of the maximal coordinate of v^A determines the motion of v^B , and vice versa. Since v_2^B is maximal throughout, $v^A(t)$ moves towards $A_2 = (0, 1, \beta)^T$ in both time intervals. In the interval $[0, t_1]$ coordinate v_1^A is maximal and $v^B(t)$ moves towards $B_1 = (-\beta, 1, 0)$; in the interval $[t_1, t_1 + t_2]$, v_3^A is maximal and $v^B(t)$ moves towards $B_3 = (1, 0, -\beta)$.

strategies 1 and 2. During this interval, player A prefers first strategy 1 and then strategy 3. We then use the rotational symmetry to determine whether this corresponds to a periodic orbit. The complete orbit consists of three such sections, with the coordinates permuted cyclically on each section.

As before, to avoid too many sub and superscripts, let $n = (n_1, n_2, n_3)^T$ be the initial value $v^A(0)$, and $m = (m_1, m_2, m_3)$ be the initial value $v^B(0)$. So the starting position given in the figure satisfies

$$n_1 > n_2, n_3 \quad \text{and} \quad m_2 = m_3 > m_1, \quad (6.25)$$

and the orbit in v^A, v^B space initially heads to respectively $(0, 1, \beta)^T = A_2$ and $(-\beta, 1, 0) = B_1$ as we require. The first time that the orbit meets Z (the indifference set) again in $t > 0$ is when the first and third coordinates of

$$v^A(t) = (1-t)n + t \begin{pmatrix} 0 \\ 1 \\ \beta \end{pmatrix} \quad (6.26)$$

become equal and player A becomes indifferent between strategies 1 and 3. Solving $v_1^A(t) = v_3^A(t)$ in (6.26) for $t = t_1 > 0$, we obtain

$$t_1 = \frac{n_1 - n_3}{n_1 - n_3 + \beta}. \quad (6.27)$$

Of course, depending on the values of the n_i it is possible that we first get that $n_1(t) = n_2(t)$ for some $t \in (0, t_1)$. Since we are not interested in this case, we insist that this does not occur and so our initial condition satisfies

$$(n_1 - n_2)\beta > (n_1 - n_3). \quad (6.28)$$

Note that the motion of v^B ensures that the largest coordinate of v^B must be v_2^B for the whole of the period $(0, t_1)$, so there is no danger that player B becomes indifferent before player A.

The v^A and v^B values at $t = t_1$ are, using (6.13),

$$v^A(t_1) = \frac{1}{(n_1 - n_3 + \beta)} \begin{pmatrix} \beta n_1 \\ \beta n_2 + n_1 - n_3 \\ \beta n_1 \end{pmatrix} \quad (6.29)$$

and

$$v^B(t_1) = \frac{1}{(n_1 - n_3 + \beta)} (\beta m_1 - \beta(n_1 - n_3), \beta m_2 + (n_1 - n_3), \beta m_3). \quad (6.30)$$

After this moment, player A changes direction and so $v^B = p^A B$ heads for $(1, 0, -\beta)$ and $t_2 > 0$ becomes the smallest number so that the first and second coordinates of $v^B(t_1 + t_2) = (1 - t_2)v^B(t_1) + t_2(1, 0, -\beta)$ become equal. This occurs when

$$t_2 = \frac{v_2^B(t_1) - v_1^B(t_1)}{v_2^B(t_1) - v_1^B(t_1) + 1} = \frac{\beta(m_2 - m_1) + (1 + \beta)(n_1 - n_3)}{\beta(m_2 - m_1) + (2 + \beta)(n_1 - n_3) + \beta}. \quad (6.31)$$

Hence, writing

$$\delta = \beta(m_2 - m_1) + (1 + \beta)(n_1 - n_3)$$

we have

$$t_2 = \frac{\delta}{\delta + \beta + n_1 - n_3}.$$

Using (6.13) again, this implies

$$v^A(t_1 + t_2) = \frac{1}{\delta + \beta + n_1 - n_3} \begin{pmatrix} n_1\beta \\ n_1 - n_3 + n_2\beta + \delta \\ n_1\beta + \beta\delta \end{pmatrix}, \quad (6.32)$$

and

$$v^B(t_1 + t_2) = \frac{1}{\delta + \beta + n_1 - n_3} ((\beta m_2 + n_1 - n_3), (\beta m_2 + n_1 - n_3), \beta(m_2 - \delta)). \quad (6.33)$$

To get an anticlockwise symmetric periodic orbit we require that

$$v^A(t_1 + t_2) = \begin{pmatrix} n_2 \\ n_3 \\ n_1 \end{pmatrix} \quad \text{and} \quad v^B(t_1 + t_2) = \begin{pmatrix} m_2 \\ m_2 \\ m_1 \end{pmatrix}. \quad (6.34)$$

Combining (6.32), (6.33) and (6.34), we need to solve the following equations:

$$\begin{aligned} n_1 \cdot \beta &= n_2 \cdot (\delta + n_1 - n_3 + \beta) \\ n_1 - n_3 + n_2 \cdot \beta + \delta &= n_3 \cdot (\delta + n_1 - n_3 + \beta) \\ n_1 \cdot \beta + \beta \cdot \delta &= n_1 \cdot (\delta + n_1 - n_3 + \beta) \\ m_2 \cdot \beta + n_1 - n_3 &= m_2 \cdot (\delta + n_1 - n_3 + \beta) \\ m_2 \cdot \beta - \beta \cdot \delta &= m_1 \cdot (\delta + n_1 - n_3 + \beta) \end{aligned} \quad (6.35)$$

and, collecting together (6.25) and (6.28), we require solutions to (6.35) that satisfy the strict inequalities

$$m_2 = m_3 > m_1, \quad n_1 > \max(n_2, n_3) \quad \text{and} \quad (n_1 - n_2)\beta > n_1 - n_3. \quad (6.36)$$

It is straightforward to check using the computer algebra package MAPLE,¹⁶ or more laboriously by hand,¹⁷ that solutions to the equalities (6.35) satisfy:

$$\begin{aligned} m_2 &= m_3 = \mu, \\ m_1 &= -\beta + 1 - 2\mu, \\ n_1 &= \beta - \mu\beta \\ n_2 &= \frac{2\beta^2 + 1 - 3\mu\beta^3 - 5\mu\beta^2 - 2\mu\beta - 2\mu + 3\mu^2\beta^2 + 3\mu^2\beta + 3\mu^2\beta^3}{\beta + 1 + \beta^2}, \\ n_3 &= -\frac{\beta^2 - \beta - 4\mu\beta^3 - 6\mu\beta^2 - 3\mu\beta - 2\mu + 3\mu^2\beta^2 + 3\mu^2\beta + 3\mu^2\beta^3}{\beta + 1 + \beta^2}, \end{aligned}$$

where μ satisfies $f_\beta(\mu) = 0$ and where

$$\begin{aligned} f_\beta(Z) &= (3\beta^2 + 3\beta + 3\beta^3) Z^3 + (-5\beta^3 - 7\beta^2 - 4\beta - 2) Z^2 + \\ &\quad + (1 + \beta + 5\beta^2 + 2\beta^3) Z - \beta^2. \end{aligned} \quad (6.37)$$

Note that for $\beta \in (0, 1]$, $f_\beta(0) = -\beta^2 < 0$ and $f_\beta(1) = -2 < 0$ while $f_\beta(1/3) = (2/9)\beta^3 + 1/9 > 0$. This implies that the cubic polynomial (6.37) always has three roots μ , two in $(0, 1)$ and one in $(1, \infty)$. When $\beta = 1$, the only of these three roots which leads to a solution satisfying the inequalities (6.36) has $\mu = 0.155\dots$, so $n_1 = 0.844\dots$, $n_2 = 0.449\dots$, $n_3 = 0.706\dots$, $m_1 = -0.311\dots$, and $m_2 = m_3 = 0.155\dots$. This solution (which depends on β) continues to exist as β decreases, and gives a periodic orbit of the desired type until one of the strict inequalities (6.36) fails to hold. Let us check what happens if one of these inequalities fails, still assuming $\beta \in (0, 1)$. If $m_1 = m_2$ then by the expressions above, $\mu = (1 - \beta)/3$. If $n_1 = n_2$ then by the first and third equations in (6.35), $\delta = 0$ and either $n_1 = n_2 = n_3$ or $n_1 = 0$ and so $\mu = 1$ (which is impossible because 1 is not a root of f_β). If $n_1 = n_3$ then the first three equations in (6.35) imply $n_1 = \beta$ or $\delta = 0$; if $n_1 = \beta$ then using the formula for n_1 we get $\beta = \beta - \mu\beta$ and so either $\beta = 0$ or $\mu = 0$ (both of which are impossible) whereas if $\delta = 0$ (and $n_1 = n_3$) then $m_1 = m_2$ and so, from the previous argument, $\mu = (1 - \beta)/3$. If $(n_1 - n_3)\beta = n_1 - n_2$ then manipulating the first three equations in (6.35) we get $1/(1 - \beta) = \beta$ (which is impossible since $\beta \in (0, 1)$) or $\delta = 0$ which in turn implies $n_1 = n_2 = n_3$ or $n_1 - n_2 + 1 = 0$ which (after some manipulations) gives $n_1 = 0$ and so $\mu = 0$ which again is impossible. In other words, the only way the inequalities can break down is when μ becomes equal to $\mu = (1 - \beta)/3$. But if we substitute $Z = (1 - \beta)/3$ into (6.37) we obtain a sixth order equation which can be factorized as

$$\frac{-1}{9}(\beta_c^2 + \beta_c - 1)(\beta_c + 1 + \beta_c^2)^2 = 0.$$

¹⁶which can be downloaded from <http://www.maths.warwick.ac.uk/~strien/Publications>

¹⁷If manipulating these equations by hand, it is useful to observe that the solution must satisfy

$$n_1 + n_2 + n_3 = 1 + \beta \quad \text{and} \quad m_1 + m_2 + m_3 = 1 - \beta$$

which come from the definitions of v^A and v^B and the fact that p^A and p^B are probability vectors.

Hence the critical value β_c of β is equal to the golden mean σ (since the other solutions of the sixth order polynomial in β are negative or complex). It is straightforward to check that for all $\beta \in (0, 1]$ the solution generated by the other root of (6.37) fails to satisfy the strict inequalities (6.36). Thus we have shown that there is unique symmetric anticlockwise periodic orbit as described in the proposition for $\beta \in (\sigma, 1]$ and none otherwise. Furthermore, the orbit shrinks down to the interior equilibrium as $\beta \downarrow \sigma$.

6.3 Stability of the anticlockwise and clockwise periodic orbits

As stated in the main text:

Proposition 6.1. *Shapley's periodic orbit is attracting for all $\beta \in [0, \sigma)$. The anticlockwise orbit which exists for $\beta \in (\sigma, 1]$ is attracting when $\beta \in (\tau, 1)$ and of saddle-type when $\beta \in (\sigma, \tau)$. Here τ is a root of a specific expression whose value is a little larger than 0.915.*

Proof. Let us just show the computation for the anticlockwise periodic orbit, because in that case an interesting bifurcation occurs. Since $\sum n_i = 1 + \beta$ and $\sum m_i = 1 - \beta$, we shall perturb the initial conditions considered in Section 6.2 above to $n'_1 = n_1 + \epsilon_1$, $n'_2 = n_2 + \epsilon_2$, $n'_3 = n_3 - \epsilon_1 - \epsilon_2$ while $m'_1 = m_1 - 2\epsilon_3$, $m'_2 = m'_3 = m_2 + \epsilon_3$. Repeating the calculation of Section 6.2 with these perturbed values we find that after slightly altered times t'_1 and t'_2 we arrive at a final position $v^A(t'_1 + t'_2)$ with coordinates $v_1^A(t_1 + t_2) + \gamma_1$, $v_2^A(t_1 + t_2) + \gamma_2$, $v_3^A(t_1 + t_2) - \gamma_1 - \gamma_2$ and a final position for $v^B(t'_1 + t'_2)$ with coordinates $v_1^B(t_1 + t_2) + \gamma_3$, $v_1^B(t_1 + t_2) + \gamma_3$, $v_3^B(t_1 + t_2) - 2\gamma_3$ where

$$\begin{pmatrix} \gamma_1 \\ \gamma_2 \\ \gamma_3 \end{pmatrix} = \frac{n_2}{n_1\beta} \begin{pmatrix} \beta(3+2\beta) - n_1 2(2+\beta) & \beta(1-n_1+\beta) - 2n_1 & 3\beta^2 - 3n_1\beta \\ \beta - 2n_2(2+\beta) & -n_2(2+\beta) & -3n_2\beta \\ 2 - \frac{2(\beta-n_1)(2+\beta)}{\beta} & 1 - \frac{(\beta-n_1)(2+\beta)}{\beta} & 3n_1 - 2\beta \end{pmatrix} \begin{pmatrix} \epsilon_1 \\ \epsilon_2 \\ \epsilon_3 \end{pmatrix}$$

plus higher order terms.¹⁸ One can compute the eigenvalues of this matrix using MAPLE; one of of them is n_2/n_1 , while the others are given as rather complicated (but exact) formulae in n_1 , n_2 and β :

$$\frac{n_2 \left(-2n_1\beta - n_1 - 2n_2 - n_2\beta + 2\beta^2 + \pm\sqrt{\Delta} \right)}{2n_1\beta}, \quad (6.38)$$

where

$$\Delta := 10n_1n_2\beta + 4n_1n_2 - 4n_2\beta^2 - 4n_2\beta^3 - 8n_1\beta^3 + 4\beta^4 + 4n_2^2 + 4n_2^2\beta + 4n_1^2\beta^2 + 4n_1^2\beta + n_2^2\beta^2 + 4n_2\beta^2n_1 - 8n_1\beta^2 + n_1^2 - 4n_2\beta - 8n_1\beta + 4\beta^2 + 4\beta^3$$

Using the explicit formulae for n_i computed in Section 6.2, and by inserting these in the expressions for the eigenvalues, we find that the eigenvalues are expressions in β . When $\beta = 1, 0.532\dots, -0.815\dots$, and $-0.184\dots$ (where the first one is n_2/n_1). One can check that as β varies the eigenvalues (6.38) always remain negative. By numerically evaluating the expressions for these (which can be done as accurately as required) we find that one of them crosses -1 when β is equal to τ where τ is roughly 0.915 while the other remains, for all $\beta \in (\sigma, 1]$, in $(-1, 0)$. Consideration

¹⁸This matrix can be deduced from equations (6.35), where it is convenient to observe that we can use the first of those equations to write $(\delta + n_1 - n_3 + \beta) = \beta n_1/n_2$.

of the sizes and signs of the eigenvalues described shows that for $\beta > \tau$ the periodic orbit is attracting, and for $\beta < \tau$ it becomes of saddle-type.

Note that we do **not** have a generic periodic doubling bifurcation¹⁹ when one of the eigenvalues becomes equal to -1 . Indeed, at this parameter the linear part of the above transformation has an eigenvector V associated to the eigenvalue -1 . However, the transition map which sends the hyperplane $m_2 = m_3$ to the hyperplane $m_1 = m_2$ is a composition of central projections (see the proof of Theorem 3.2. In particular, it sends the line through V to the line through V (remember V is an eigenvector) and it is a linear fractional transformation on this line with derivative -1 at the fixed point. But taking a map of the form $f(x) = -x + \alpha x^2 + \gamma x^3 + \dots$ we always have $f^2(x) = x + 0x^2 + (?)x^3$. So in our case we get that the second iterate of the linear fractional transformation is equal to the identity map up to second order at the fixed point. But this implies that it is in fact equal to the identity map. So instead of a generic periodic doubling bifurcation, in this case we get non-generic dynamics at the bifurcation parameter $\beta = \tau$; at this parameter value there is one-parameter family (continuum) of periodic orbits.

The computation showing that Shapley's periodic orbit is attracting for all $\beta \in (0, \sigma)$ goes similarly. \square

6.4 Dynamics and a periodic orbit on the set J

We will now consider, again using v^A, v^B space, the flow on the codimension two indifference set J defined in the main text. Recall that the flow which remains on J is the unique continuous extension to J of the flow off J , everywhere except at the interior equilibrium.

Proposition 6.2. *The system has a Hopf-like bifurcation when $\beta = \sigma$ on the topological two-dimensional manifold J . The orbits on J spiral towards the interior equilibrium $E = (E^A, E^B)$ when $\beta \in (0, \sigma]$ while for $\beta \in (\sigma, 1]$ all orbits in J (except the one remaining at E) tend to a periodic orbit Γ on J .*

Proof. Again we compute a segment of orbit which makes one third of a complete rotation around the interior equilibrium, and use the rotational symmetry to compute the whole orbit. We take an initial condition $v^A = n$ and $v^B = m$ where $n_2 = n_3 > n_1$ and $m_1 = m_2 = m_3 = (1 - \beta/3)$.

Player A (whose preferences depend on v^A) is at first indifferent between strategies 2 and 3, and so adjusts p^A towards some convex combination of P_2 and P_3 , implying that v^B moves towards the same convex combination of B_2 and B_3 . The convex combination

$$\frac{(1 + \beta)}{(2 + \beta)} B_2 + \frac{1}{(2 + \beta)} B_3 = \frac{1}{(2 + \beta)} (1, -\beta(1 + \beta), 1) \quad (6.39)$$

is chosen so that the orbit remains in J , i.e. so that $v_1^B(t) = v_3^B(t)$ in $t > 0$. (We stress again that this is not in any sense an arbitrary choice; it is the unique choice giving a continuous extension of the flow defined off the codimension two indifference surface.) Consequently player B will, for $t > 0$, be indifferent between strategies 1 and 3, will adjust p^B towards some convex combination of P_1^B and P_3^B , and so v^A will move towards the same convex combination of A_1 and A_3 . In this case, the combination

$$\frac{1}{(1 + \beta)} A_1 + \frac{\beta}{(1 + \beta)} A_3 = \frac{1}{(1 + \beta)} (1 + \beta^2, \beta, \beta)^T \quad (6.40)$$

¹⁹as would be expected in a normal differential equation

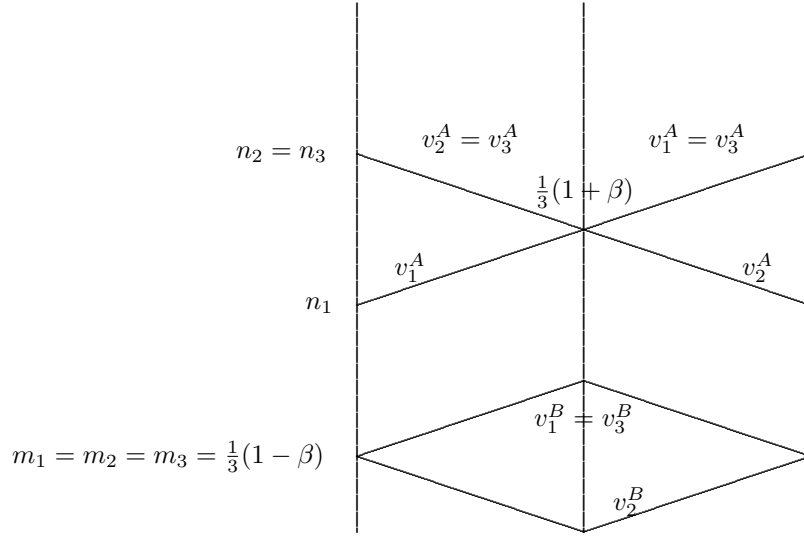


Figure 11: Part of the periodic orbit on J with (v^A, v^B) plotted against time.

is chosen so that $v_2^A(t) = v_3^A(t)$ in $t > 0$.

This motion continues until a time $t_1 \in (0, 1)$ at which $v_1^A(t_1) = v_2^A(t_1) = v_3^A(t_1) = \frac{1}{3}(1 + \beta)$ so that t_1 satisfies, using (6.13) and (6.40)

$$v^A(t_1) = (1 - t_1)v^A(0) + t_1 \frac{1}{1 + \beta} \begin{pmatrix} 1 + \beta^2 \\ \beta \\ \beta \end{pmatrix} = \frac{1 + \beta}{3} \begin{pmatrix} 1 \\ 1 \\ 1 \end{pmatrix}.$$

Hence

$$t_1 = \frac{(n_2 - n_1)(1 + \beta)}{(n_2 - n_1)(1 + \beta) + (1 + \beta^2 - \beta)}.$$

We have also, from (6.13) and (6.39),

$$v^B(t_1) = v^B(0)(1 - t_1) + t_1 \frac{1}{2 + \beta} (1, -\beta - \beta^2, 1).$$

Now since $v_i^B(0) = (1 - \beta)/3$ for $i = 1, 2, 3$, we have

$$v_1^B(t_1) - v_2^B(t_1) = \frac{t_1}{2 + \beta} [1 + \beta + \beta^2]. \quad (6.41)$$

Player A now becomes indifferent between strategies 1 and 3, while player B is still indifferent between strategies 1 and 3 (inspection shows this is the only way to remain on J). In the interval $t \in (t_1, t_1 + t_2)$ we have that $v^A(t)$ heads for

$$\frac{(1 - \beta)}{(2 - \beta)} A_1 + \frac{1}{(2 - \beta)} A_3 = \frac{1}{(2 - \beta)} (1, \beta(1 - \beta), 1)^T \quad (6.42)$$

and $v^B(t)$ heads for

$$\frac{(1+\beta)}{(1+2\beta)}B_1 + \frac{\beta}{(1+2\beta)}B_3 = \frac{1}{(1+2\beta)}(-\beta^2, 1+\beta, -\beta^2). \quad (6.43)$$

Using (6.13) and (6.43) we seek to compute t_2 such that $v^B(t_1 + t_2) = \frac{(1-\beta)}{3}(1, 1, 1)$. This gives

$$t_2 \left[\frac{1}{(1+2\beta)}(-\beta^2, 1+\beta, -\beta^2) - v^B(t_1) \right] = \frac{1}{3}(1-\beta)(1, 1, 1) - v^B(t_1)$$

which implies

$$t_2 = \frac{v_1^B(t_1) - v_2^B(t_1)}{\frac{1+\beta+\beta^2}{1+2\beta} + v_1^B(t_1) - v_2^B(t_1)} = \frac{t_1(1+2\beta)}{t_1(1+2\beta) + (2+\beta)}.$$

Now (6.13), (6.42) and the fact that all components of $v^A(t_1)$ are equal imply that

$$v_1^A(t_1 + t_2) - v_2^A(t_1 + t_2) = \frac{t_2}{2-\beta} [1 - \beta + \beta^2].$$

Substituting in for t_2 and then for t_1 we obtain

$$\begin{aligned} v_1^A(t_1 + t_2) - v_2^A(t_1 + t_2) &= \frac{t_1(1+2\beta)}{(t_1(1+2\beta) + (2+\beta))} \frac{(1-\beta + \beta^2)}{(2-\beta)} = \\ &= \frac{(n_2 - n_1)}{(n_2 - n_1)3(1+\beta)^2 + (2+\beta)(1-\beta + \beta^2)} \frac{(1+\beta)(1+2\beta)(1-\beta + \beta^2)}{(2-\beta)}. \end{aligned}$$

This formula gives us the value of $|v_1^A(t) - v_2^A(t)|$ at the end of the two legs, as a function $F()$ of the initial value $|n_2 - n_1|$, where

$$F(X) := \frac{X(1+\beta)(1+2\beta)(1-\beta + \beta^2)}{(2-\beta)(3(1+\beta)^2X + (2+\beta)(1+\beta^2 - \beta))}.$$

Now F is a linear fractional transformation $F(X) = \frac{aX}{bX+c}$ and

$$F'(0) = \frac{a}{c} = \frac{(1+\beta)(1+2\beta)(1-\beta + \beta^2)}{(2-\beta)(2+\beta)(1-\beta + \beta^2)} = \frac{2\beta^2 + 3\beta + 1}{-\beta^2 + 4}$$

which is less than 1 when $\beta < \sigma$ and greater than 1 when $\beta > \sigma$. Since $F(X) \rightarrow 1$ as $X \rightarrow \infty$, this implies that $x \mapsto F(x)$ has zero as an attracting fixed point when $\beta \in (0, \sigma]$, and there exists an attracting fixed point $x > 0$ of F when $\beta > \sigma$. This solution x corresponds to the value of $n_2 - n_1$ for which there is an associated periodic orbit Γ on J . This orbit attracts all orbits on J except the one starting at the interior equilibrium (E^A, E^B) .

To prove the last part of the proposition, note that $F(X) = X$ is equivalent to

$$X = \frac{(1+\beta^2 - \beta)(\beta^2 + \beta - 1)}{(2-\beta)(1+\beta)^2}.$$

Now for the initial condition n on Γ , we have $n_2 - n_1 = X = F(X)$, $n_2 = n_3$, and $n_1 + n_2 + n_3 = (1+\beta)$. Hence $n_1 = \frac{-2X+1+\beta}{3}$. Note that on the line $Z_{1,3}^A$ in Σ_B (see Figure 9 in the main text) one

has (in p^B coordinates) $Q_{1,3}^B = \frac{1}{1+\beta}(\beta, 1 + \beta^2, \beta)$, $E^B = \frac{1+\beta}{3}(1, 1, 1)$ and $R_{1,3}^B = \frac{1}{2-\beta}(1, \beta - \beta^2, 1)$ (and symmetrically for other points). During the third of the orbit studied we have that we travel first along $[R_{23}^B, E^B]$ until meeting E^B and then along $[E^B, R_{13}^B]$. The proportion

$$\frac{|E_{23}^B - f_{23}^B|}{|Q_{23}^B - f_{23}^B|}$$

is therefore, (by doing the computations in the p^B -simplex)

$$\frac{\frac{1+\beta}{3} - n_1}{\frac{1+\beta^2}{1+\beta} - n_1} = \frac{\frac{1+\beta}{3} - \frac{-2X+1+\beta}{3}}{\frac{1+\beta^2}{1+\beta} - \frac{-2X+1+\beta}{3}} = \frac{\beta^2 + \beta - 1}{2\beta + 1}.$$

So when β is equal to the golden mean then this is equal to 0 and it increases monotonically when $\beta \in [\sigma, 1]$ (its maximum is $1/3$). Similarly,

$$\frac{|f_{23}^B - E_{23}^B|}{|R_{23}^B - E_{23}^B|} = \frac{\frac{1+\beta}{3} - n_1}{\frac{1+\beta}{3} - \frac{\beta-\beta^2}{2-\beta}} = \frac{\frac{1+\beta}{3} - \frac{-2X+1+\beta}{3}}{\frac{1+\beta}{3} - \frac{\beta-\beta^2}{2-\beta}} = \frac{\beta^2 + \beta - 1}{(1 + \beta)^2}$$

(which again increases in β). □

Note that when $\beta \neq \sigma$, the time taken for a trajectory on J to spiral into or out of the interior equilibrium E is finite. This is because for small X we have that $F(X) = c_1(\beta)X + O(X^2)$ and that the time taken for this step is $t_1 + t_2 = c_2(\beta)X + O(X^2)$ for some constants $c_1(\beta)$, $c_2(\beta)$ depending on β . When $c_1(\beta) \neq 1$, which is true precisely when $\beta \neq \sigma$, this gives geometric (rather than exponential) convergence towards or divergence away from E . This phenomenon is intimately connected with the fact that the flow does not extend in a continuous way to E ; there is genuine non-uniqueness of the flow at E (since trajectories may remain at E for all positive and negative time, or may leave it at some moment in positive time ($\beta > \sigma$) or in negative time ($\beta < \sigma$)). When $\beta = \sigma$ the time taken for trajectories to tend to E is infinite, as can easily be checked.